# JOURNAL OF THE AERONAUTICAL SCIENCES

VOLUME 1 NUMBER 4

OCTOBER, 1934

*Published by the*

INSTITUTE OF THE AERONAUTICAL SCIENCES, INC.

*with the cooperation of the*

AMERICAN INSTITUTE OF PHYSICS
Incorporated

# INSTITUTE OF THE AERONAUTICAL SCIENCES, INC.

OFFICERS

AND

EDITORIAL BOARD

*President*
CHARLES L. LAWRANCE

*Vice-President*
D. W. DOUGLAS

*Vice-President*
LESSITER C. MILBURN

*Treasurer*
EDWIN E. ALDRIN

*Secretary*
LESTER D. GARDNER

COUNCIL

E. E. ALDRIN
J. S. AMES
V. E. CLARK
J. C. HUNSAKER
JAMES H. KIMBALL
CHARLES L. LAWRANCE
GROVER LOENING
GEORGE J. MEAD
ARTHUR NUTT
ELMER A. SPERRY, JR.
EDWARD P. WARNER
T. P. WRIGHT


---

# JOURNAL OF THE AERONAUTICAL SCIENCES


VOL. 1 OCTOBER, 1934 NO. 4

*Editor:* J. C. HUNSAKER, *Massachusetts Institute of Technology*

PUBLISHED QUARTERLY BY THE INSTITUTE OF THE AERONAUTICAL SCIENCES, INC., AT PRINCE AND LEMON STREETS, LANCASTER, PENNSYLVANIA.


The JOURNAL OF THE AERONAUTICAL SCIENCES is the official publication of the Institute of the Aeronautical Sciences, Inc., and is devoted to papers on experimental, theoretical, and applied science as employed in aeronautics.

Manuscripts for publication, proofs, and all correspondence should be addressed to the Editorial Secretary of the JOURNAL. Subscription price: $2.00 per year; single copies, 50¢. Foreign subscription price: $3.00 per year; single copies, 75¢. Advertising rates will be sent on application.

Correspondence regarding advertising and subscriptions may be addressed to Publication Office, Prince and Lemon Streets, Lancaster, Pennsylvania, or to Editorial Office of the JOURNAL OF THE AERONAUTICAL SCIENCES, 5431 R. C. A. Building, Rockefeller Center, New York, New York.

---


Entered as second class matter, January 9, 1934, at the post office at Lancaster, Pa.
Acceptance for mailing at a special rate of postage provided for in the Act of October 3, 1917, embodied in paragraph 4, section 412, P. L. & R., authorized February 17, 1934

JOURNAL OF THE AERONAUTICAL SCIENCES

Volume 1 OCTOBER, 1934 Number 4

# Servo Control Flaps

ELLIOTT G. REID, *Stanford University*

(Received August 9, 1934)

## INTRODUCTION

THE device now known as the servo control flap is a development of the "Flettner rudder" which was invented by the designer of the rotor ships. First applied to a European merchant vessel in 1921,[1] the servo rudder was so satisfactory that at least twenty-five sea-going ships had been similarly equipped by 1926.

One of these early rudders is shown in Fig. 1. The rudder is free to swing about its post whereas the orientation of the auxiliary flap with respect to the rudder is manually controlled by the helmsman through the action of a cam and rocker mechanism. The principle of operation is readily understood by considering the equilibrium of the effectively rigid assembly of rudder and flap. With the ship under way, the assembly assumes the position in which the resultant moment about the rudder post is zero. A transverse force acts on the assembly whenever the flap is displaced from its neutral position because the moment of the large force acting upon the rudder is equilibrated by that of a much smaller force which acts upon the more distant servo flap.

The flap shown in Fig. 2 is a balancing device which is operated by movement of the rudder; when the rudder is put to starboard, the flap, which is linked to a fixed arm on the sternpost, turns to port and thus contributes balancing moments which are of such magnitude as to reduce greatly the necessary steering engine power. The development of this second function of the servo flap is of interest because the same cycle appears to have been followed in aeronautic application.

The servo flap has been used on ships only as a servo rudder and as a rudder balance. These uses have been duplicated in aeronautic practice but, in addition, a third function of the servo flap has been discovered. The "trimmer" consists of an auxiliary flap set into or attached to the main flap of a control surface and which can be set at any desired angle with respect to the latter by the operation of an irreversible, auxiliary control. Originated as a substitute for the conventional adjustable stabilizer, trimmers are now found on rudders and ailerons, as well, where they serve to accomplish, in flight, the results previously obtainable by offsetting the fin or re-rigging a wing, both of which could be done only on the ground. Besides the structural advantages of fixed stabilizers and fins over adjustable ones, the trimmers offer as well, a solution of the problem of keeping a multi-engine machine on a straight course without great effort in the event of failure of one power plant and they make it

[1] Olav Overgaard, and J. Livingston, *Recent Development of the Ship Rudder with Particular Reference to the "Flettner Rudder,"* Trans. Soc. Nav. Arch. and Mar. Eng. **34**, 205 (1926).

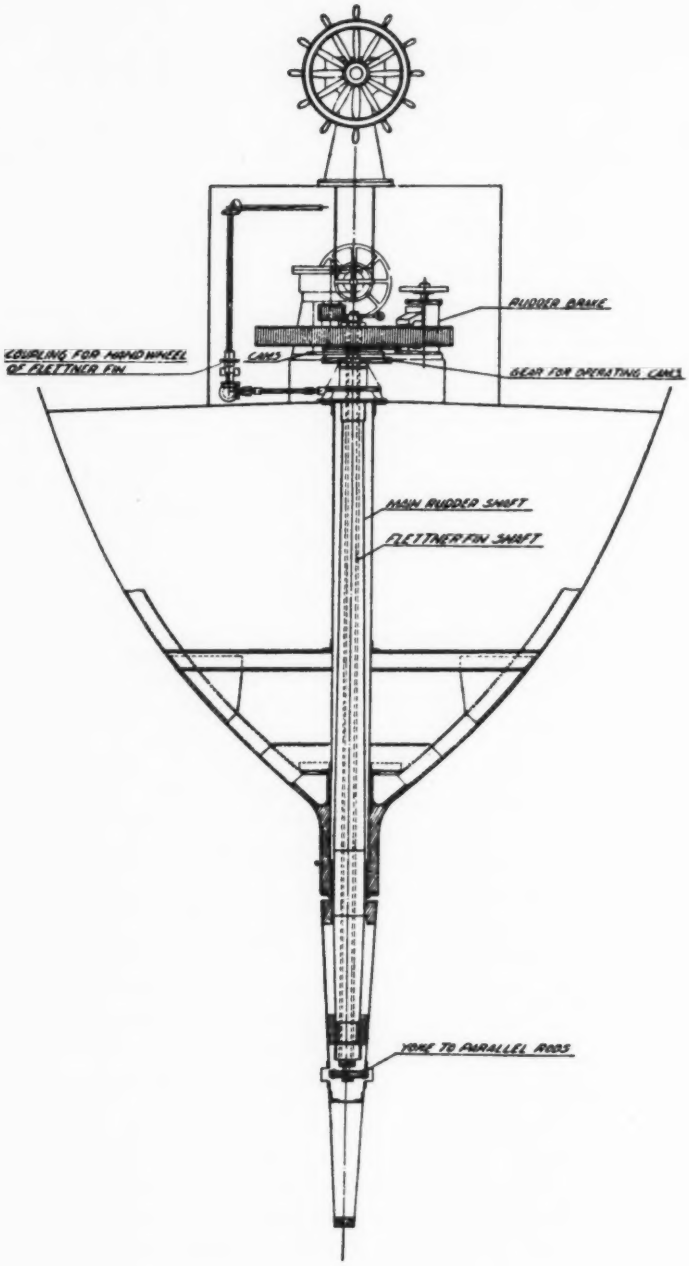


(a)

FIG. 1. (See also next page.)

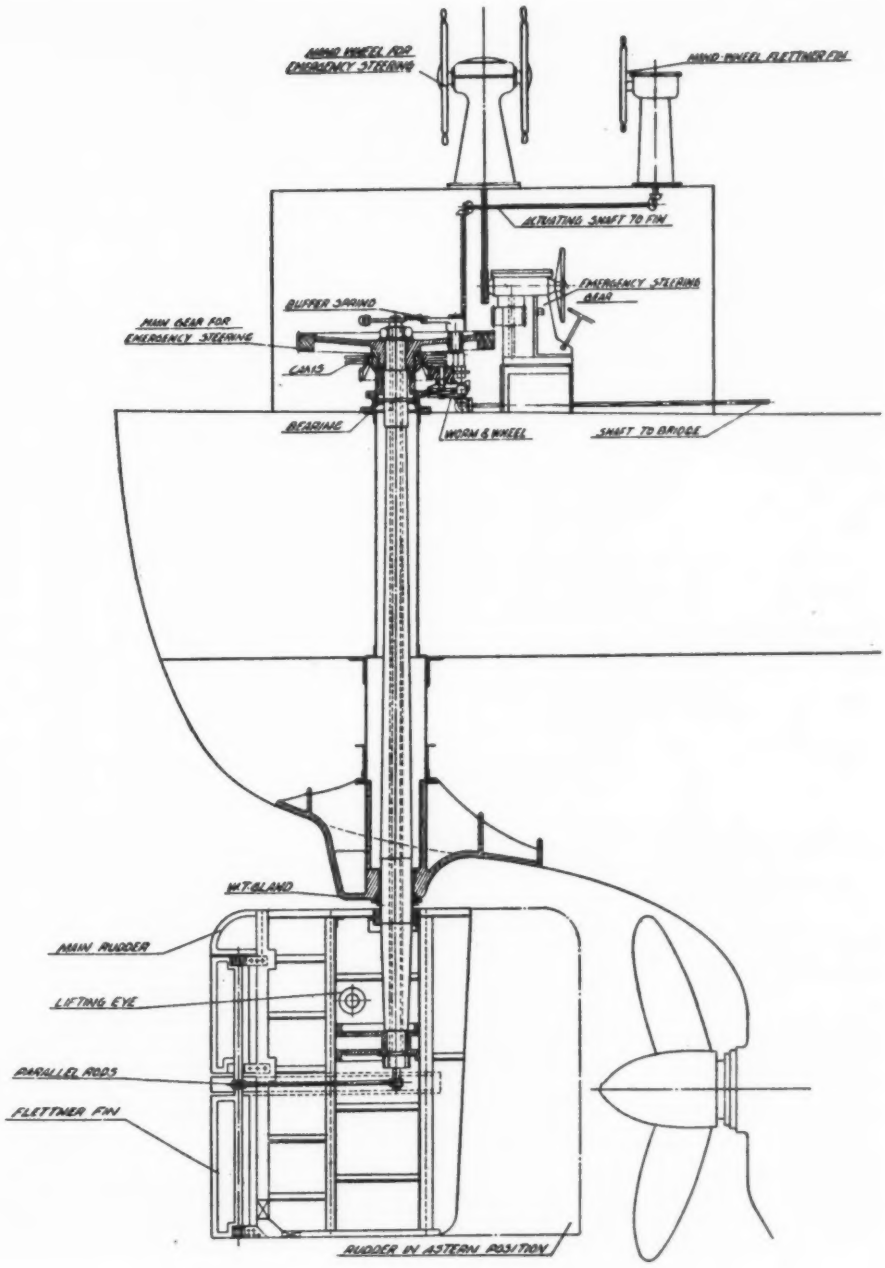


(b)

FIG. 1. Reproduction of plate 115, Trans. Soc. Nav. Arch. and Mar. Eng., Vol. 34, 1926.

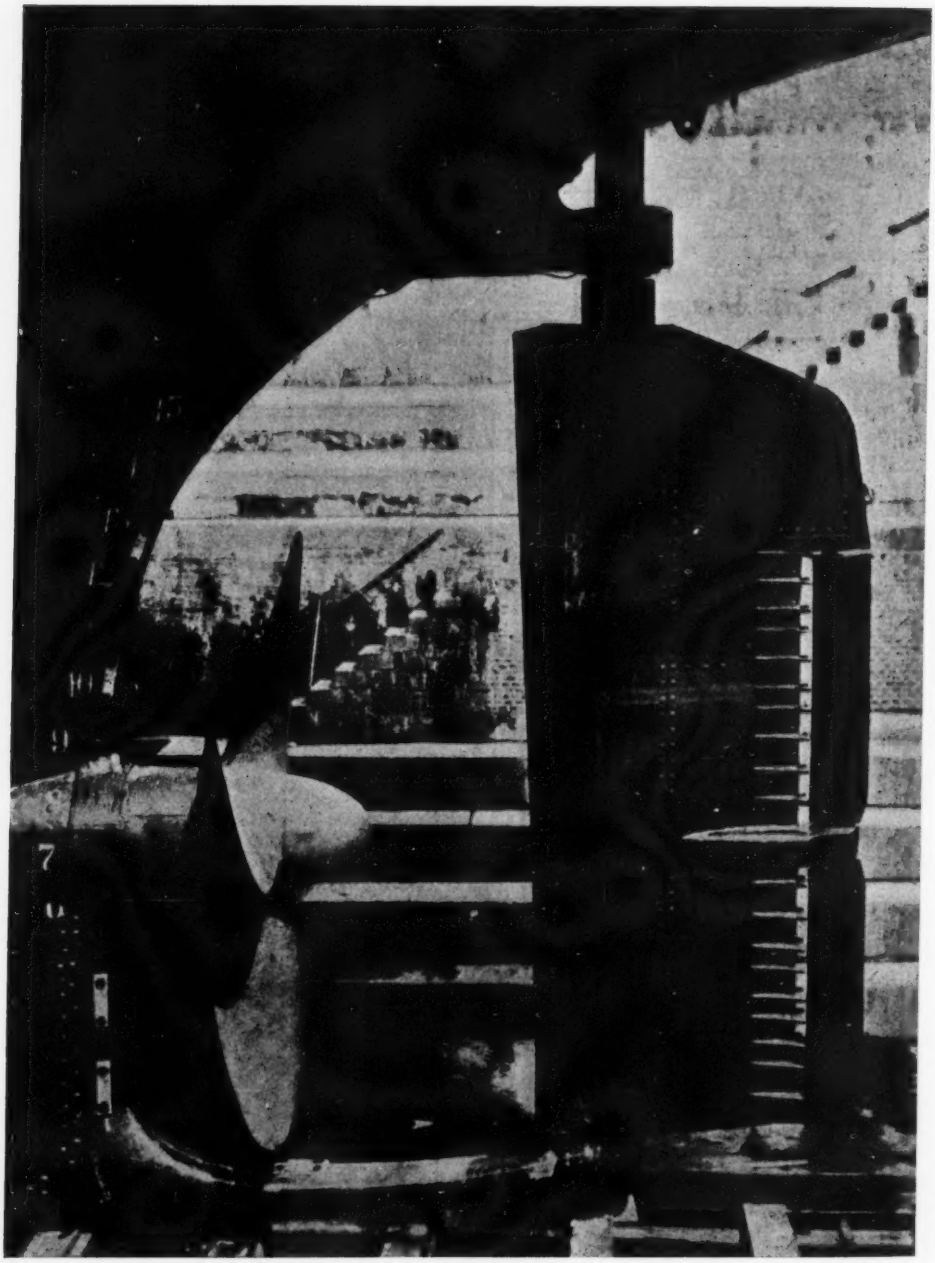

FIG. 2. Reproduction of plate 117, Trans. Soc. Nav. Arch. and Mar. Eng., Vol. 34, 1926.

possible to keep an unsymmetrically loaded or "wing heavy" machine in lateral trim without muscular effort on the part of the pilot.

It appears that the British were among the first to experiment with the servo rudder for airplanes. A D.H.10 was fitted with a servo rudder in 1926 or 1927; since then, a number of large British machines have been similarly equipped.* In this country a few trimotors have had servo rudder balances but, so far as the writer knows, no American airplane has ever used a servo flap as the only means of operating a principal control surface. About three years ago, successful experiments with trimmers were carried out in several countries; today, trimming flaps are being used in the control surfaces of all sorts of airplanes throughout the world.

In spite of the now numerous and promising applications of servo flaps, a meager amount of information concerning their properties is available. The only relevant material known to the writer consists of a study of a servo operated, "all moving" rudder,[2] i.e., one intended for use with no fin, the results of tests of a few non-related models of servo control surfaces designed for specific airplanes[3] and one investigation of a servo flap balance.[4] It thus appears that the practical application of this device has preceded any thorough investigation of its aerodynamic characteristics.

Several questions need to be answered if designers are to make intelligent use of servo control flaps. Outstanding among them are the following:

(a) What effect has servo aspect ratio upon the range and efficiency of control?
(b) What effect has servo area upon the same qualities?
(c) Is it necessary or advantageous to balance the main flap of a servo operated control surface?
(d) If balance is desirable, what form should the balance take?

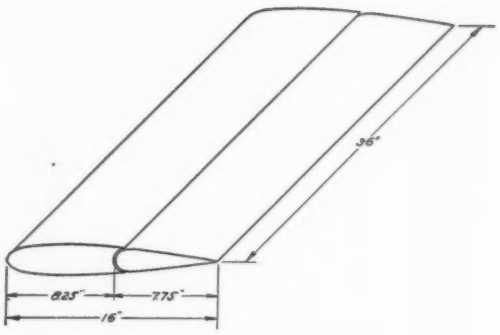


FIG. 3.

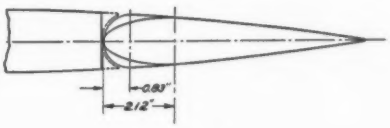


FIG. 4.

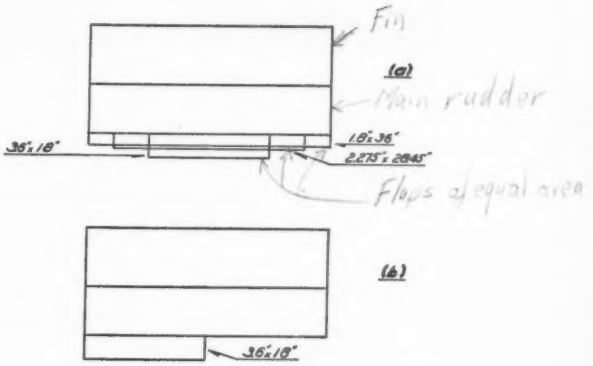


FIG. 5. Servo control flaps; plan views.

FIG. 6.

* Blackburn "Iris" and "Sydney," Beardmore "Inflexible," Fairey Long Range Monoplane, SARO "A-7," Short "Calcutta," "Kent," "Rangoon" and "Valetta."

[2] K. V. Wright, *Wind Tunnel Tests of Various Servo Rudder Systems*, Advisory Committee for Aeronautics (Great Britain), R. and M. No. 1186, 1928.

[3] F. B. Bradfield, *A Collection of Wind Tunnel Data on the Balanicng of Controls*, Advisory Committee for Aeronautics (Great Britain), R. and M. No. 1420, 1931.

[4] Léon Kirste, *Étude sur les Gouvernails Compensés*, Thesis, Universite de Paris, 1932.

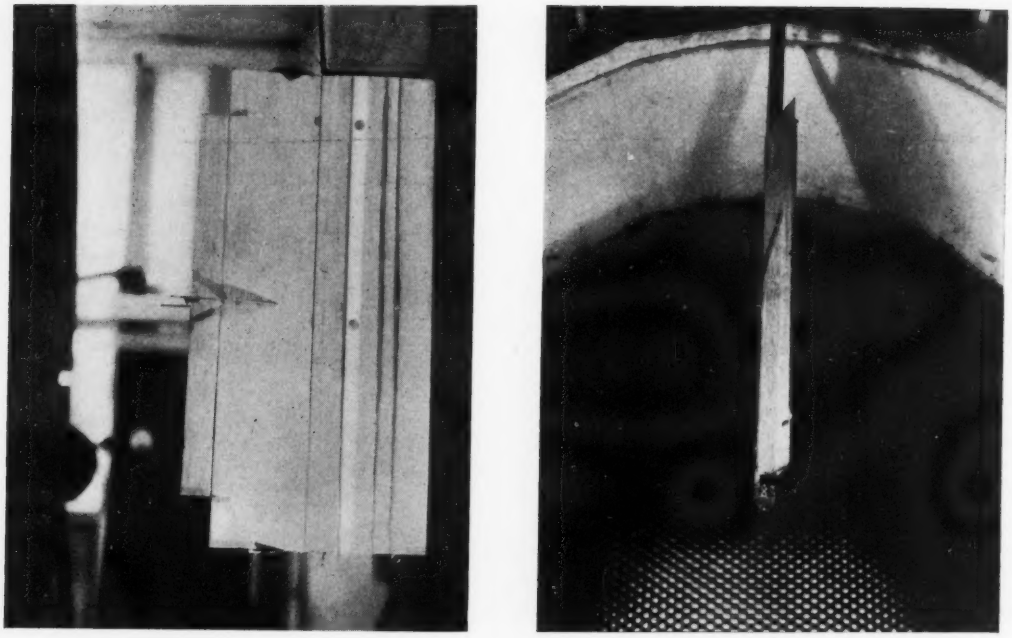

(a) (b)

FIG. 7.

(e) Does it appear probable that servo controls may be more satisfactory for very large aircraft than aerodynamically balanced, manually operated ones?

The results which are presented in this paper are taken from the Engineers' theses of two Stanford graduate students.[5, 6] While the experimental information is not sufficiently comprehensive to furnish complete answers to all the foregoing questions, considerable light is shed upon each one.

## MODELS AND APPARATUS

The control surface to which the various servo flaps were applied is shown in Fig. 3; its profile is the N.A.C.A. M-3. The modifications made for the tests of balanced flaps are shown in Fig. 4. The dimensions of the servo flaps (of M-3 profile) and their positions with respect to the main flap are illustrated by Fig. 5. The original unbalanced flap was supported on pivot and socket bearings; the balanced flaps were hung in the adjustable ball bearing hinges shown in Fig. 6.

The tests were made in the 8 ft., open throat wind tunnel of the Daniel Guggenheim Aeronautic Laboratory at Stanford University. The force and hinge moment experiments were made by use of a conventional form of wire balance.

The only special apparatus used in the investigation was an optical measuring instrument which made it possible to determine the angular positions of the main and servo flaps while floating freely behind the fixed surface in the wind stream.

## EXPERIMENTAL METHODS AND PROCEDURE

All of the tests described below were made with the forward part of the control surface (stabilizer) at zero degrees angle of attack.

The basic or reference data were obtained by testing the model in its various forms without any servo flap, i.e., as though it were intended

[5] Leo J. Devlin, Jr., *An Investigation of Servo Control Systems for Aircraft*, Thesis, Stanford University, December, 1932.

[6] Daniel B. Woodyatt, *A Study of Servo Operated Balanced Control Surfaces*, Thesis, Stanford University, December, 1933.

for direct manual operation. The lifts and drags corresponding to flap angles from zero up to at least 30 degrees were measured in each case.

The method of testing the servo-equipped control surface was to determine the angular displacements of the main flap for each one of a series of servo settings and then to lock the movable parts in the positions so determined and to measure the forces experienced under these conditions. The basis for this procedure is, of course, the assumption that the pilot of an airplane will exercise control over the displacement of the servo flap with respect to the main flap.

To determine the equilibrium or "floating angles," the model was mounted vertically in the tunnel as illustrated by Fig. 7, the servo set at a known angle with respect to the flap and the angular displacement of the main flap with respect to the stabilizer under the action of the wind forces determined by use of the optical instrument previously mentioned. A complete run of this kind was made for each servo installation, the servo angles being increased in each case until increasing displacements resulted in reduction of the flap angle. During the force tests, both the main and servo flaps were locked in the positions determined in the floating angle tests. This procedure was adopted in order to eliminate the necessity for statically balancing each flap-servo combination.

## Combinations Tested

The combinations tested with the unbalanced main flap are illustrated in Fig. 5. Group (a), three servos of the same area, yielded data concerning the effects of aspect ratio. The installation (b) was made to isolate a suspected "tip effect." The servos shown in (c) have equal areas; they were obtained by removing the tips of the two narrow servos shown in (a). The tests of group (c) furnished information on the effects of servo area, confirmed the suspicion of "tip effect" and supplemented the aspect ratio results obtained from (a).

Additional tests were made to determine whether a beneficial slot effect might be obtained by moving the hinge axis of the servo aft of the leading edge. This involved hinging the symmetrically located servo of smallest aspect ratio at 0.15 and 0.25 chord aft of its leading edge.

Tests of balanced control flaps were necessarily preceded by consideration of the known methods of achieving aerodynamic balance. The overhanging horn type of balance was eliminated on account of its non-uniform action. The forward projecting outrigger airfoil balance and its derivative, the Dornier linked auxiliary airfoil, were discarded as being too complicated and not sufficiently powerful unless supplemented by the use of an inset hinge. The use of an inset hinge as the method of balancing the flap was chosen as the best combination of power, efficiency, uniformity of action and structural simplicity.

Hinge moment tests were made in order to select satisfactory positions for the hinges of the balanced flaps. The positions finally selected were such that both the round and elliptical nosed flaps were under-balanced by approximately equal amounts. Only one servo (1.8″ $\times$28.45″) was applied to each of the balanced flaps.

All force tests were made at an airspeed of 65 miles per hour.

## Results

The results are presented in graphical form in Figs. 8 to 18. The symbols for flap and servo displacements are indicated on the first figure. The area of the main control surface without servo, 4 sq. ft., was used in all coefficient calculations. Direct comparison is thus facilitated as the coefficients are directly proportional to the total forces experienced by the several assemblies.

## Discussion

The tests of the 0.45 sq. ft. servos shown in Fig. 5(a) revealed that the servo which extends across the whole span is capable of deflecting the main flap by the greatest amount and that as the aspect ratio is reduced so are the maximum flap deflections (Fig. 8(a)). It is noteworthy that differences of any consequence are confined to large flap angles and that they increase as the span of the servo approaches that of the flap. The same statements are equally true of the corresponding curves of lift coefficient *vs.* flap

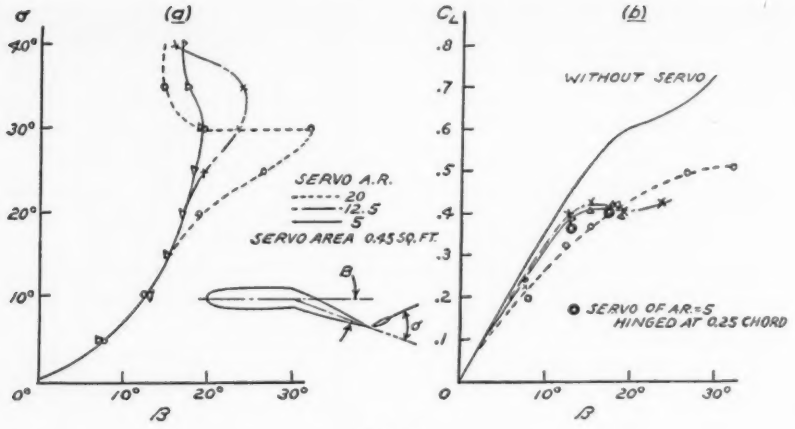


FIG. 8.

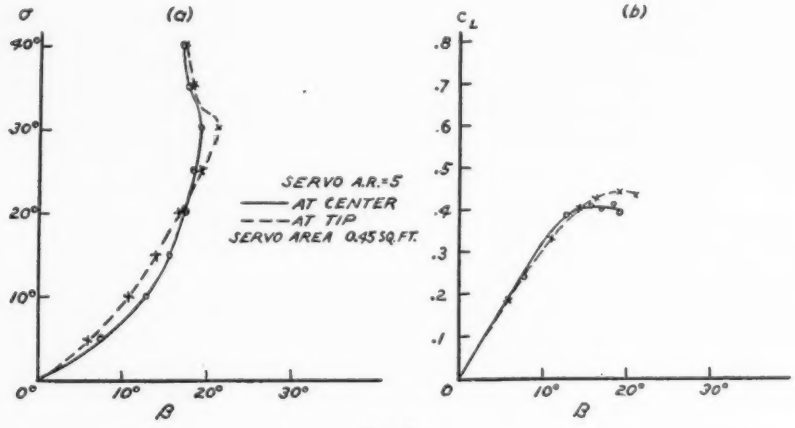


FIG. 9.

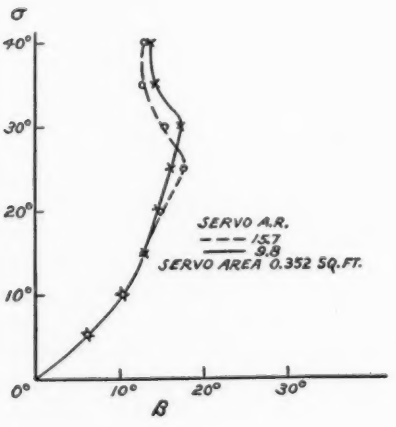


FIG. 10.

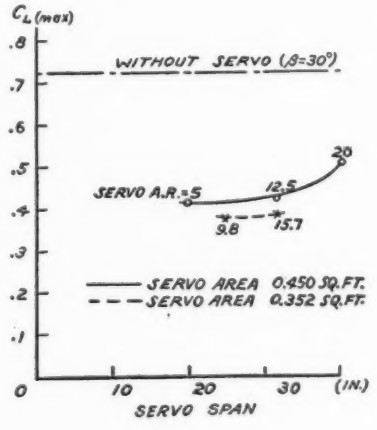


FIG. 11.

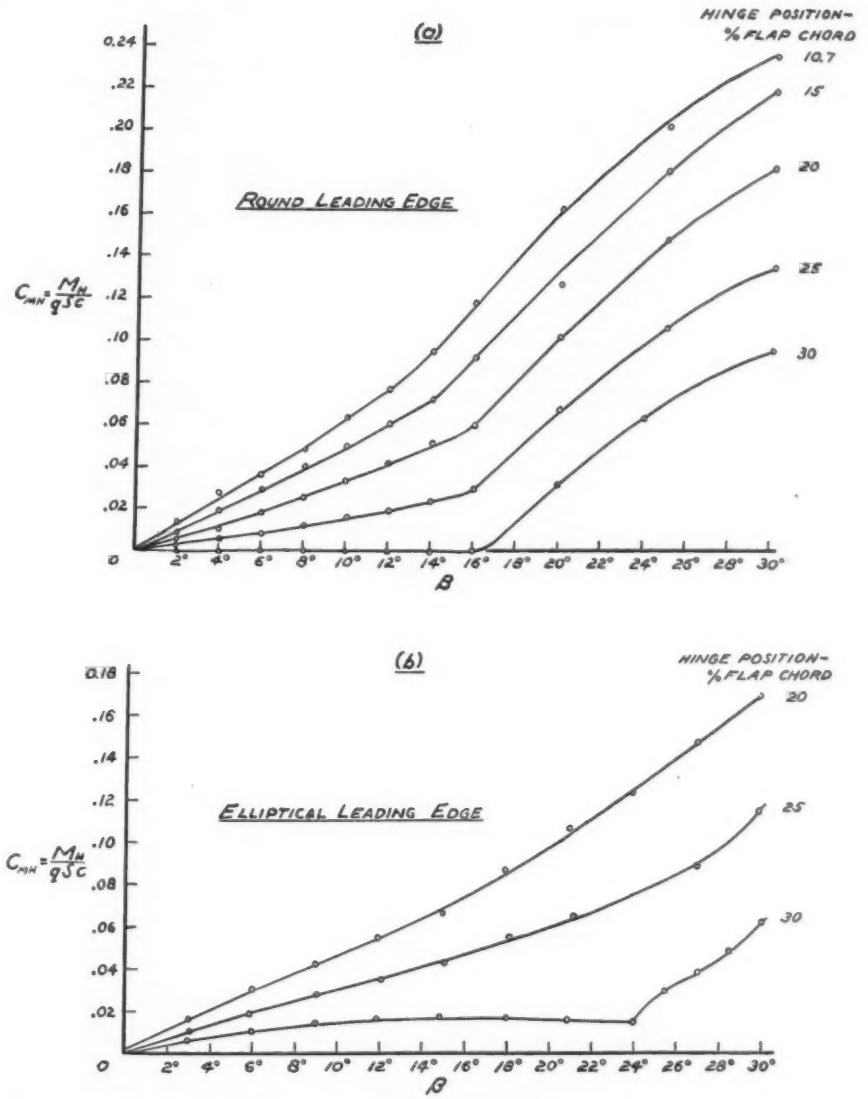
(a)
HINGE POSITION-
% FLAP CHORD
10.7
15
20
25
30
ROUND LEADING EDGE
$C_{MH} = \frac{M_H}{qSc}$
0.24
.22
.20
.18
.16
.14
.12
.10
.08
.06
.04
.02
0
2° 4° 6° 8° 10° 12° 14° 16° 18° 20° 22° 24° 26° 28° 30°
β
(b)
HINGE POSITION-
% FLAP CHORD
20
25
30
ELLIPTICAL LEADING EDGE
$C_{MH} = \frac{M_H}{qSc}$
0.18
.16
.14
.12
.10
.08
.06
.04
.02
0
2° 4° 6° 8° 10° 12° 14° 16° 18° 20° 22° 24° 26° 28° 30°
β

FIG. 12.

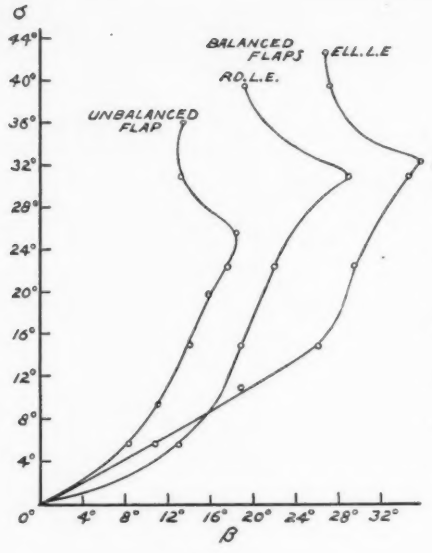


FIG. 13.

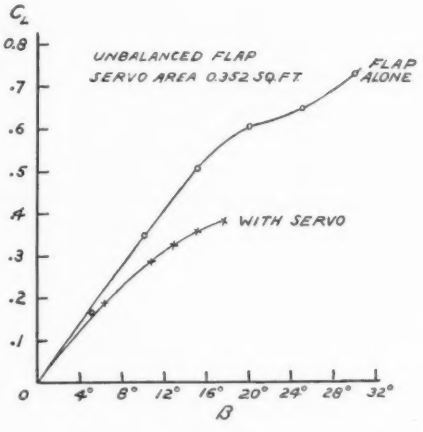


FIG. 14.

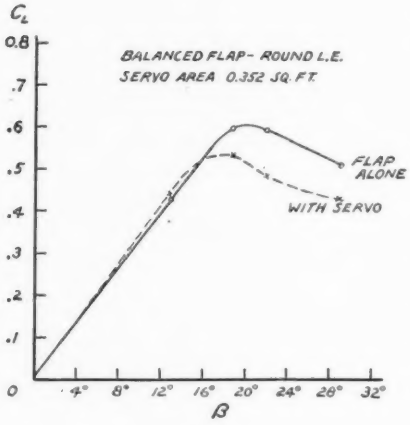


FIG. 15.

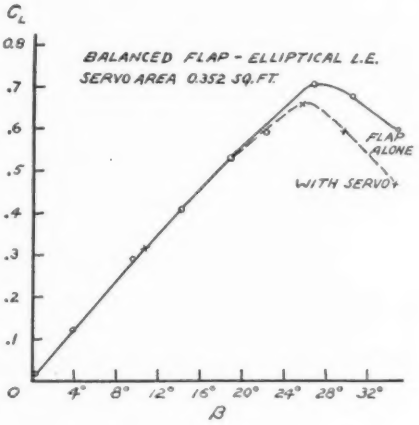


FIG. 16.

angle (Fig. 8(b)). These circumstances suggested that the differences might have their origin in the character of the airflow around the tips of the main surface rather than in the flow around the servo itself.

In an effort to isolate this phenomenon, the servo of aspect ratio five was transferred from its symmetrical position to the one shown in Fig. 5(b). The floating angles and lifts obtained with these two arrangements are shown in Fig. 9. It is apparent that the servo produces larger displacements of the flap and, consequently, larger lift coefficients when it operates in the wake of the tip of the main surface. To confirm this qualitative indication, two symmetrically located servos of reduced span and 0.352 sq. ft. area

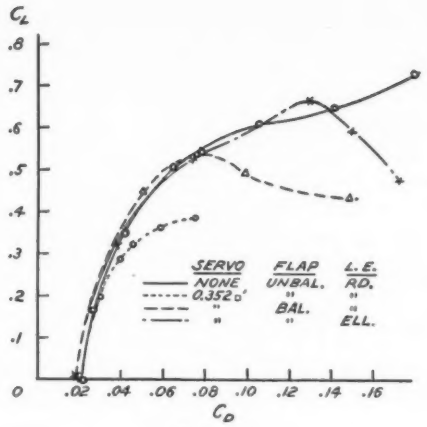


FIG. 17.

(Fig. 5(c)) were tested. The floating angles are shown in Fig. 10. It will be seen that although the curves are not identical, the maximum flap displacements differ negligibly. The lift curves are not reproduced but the small difference between the maximum values is shown in Fig. 11.

The curves of this same figure clearly show that changing the servo aspect ratio from 5 to 12 or 15 has an extremely small effect upon the maximum lift coefficient of the control surface provided that the servo span does not exceed 80 percent of the control surface span. It may be noted in passing that servo tip effect has little significance in modern design since rectangular or square tipped airfoils are now so carefully avoided.

The information concerning servo area is rather meager. The maximum lift coefficients for servos of 0.45 and 0.352 sq. ft. (0.232 and 0.182 main flap area) are plotted in Fig. 11. Within the span limits common to both curves, the ratio of the maximum lift coefficients is approximately 1.11 while the ratio of the servo areas is 1.28. The drawing of general conclusions from such scanty data is not justified but, at least for the range of combinations used in these tests, it is clear that the maximum lift coefficient increases less rapidly than in direct proportion to the servo area.

The beneficial slot effect sought by insetting the servo hinge was not to be found. The floating angles were practically unaffected by servo hinge position and the lifts measured under equilibrium conditions showed a slight adverse effect. For this reason, complete curves are not presented; two specially designated spots in Fig. 8(b) illustrate the effect of setting the servo hinge back to the 0.25 chord position.

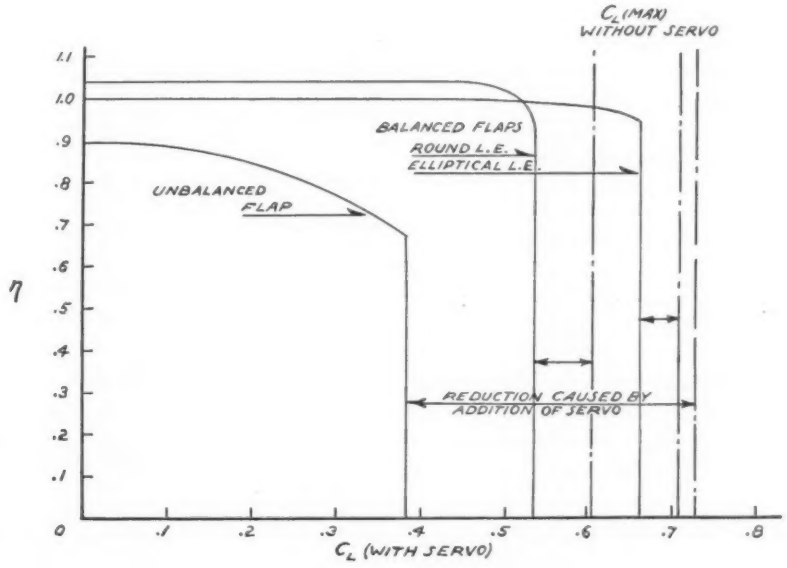


FIG. 18.

The results of the hinge moment measurements made with the balanced main flaps are presented in Fig. 12. Although hinge moments were measured only with the stabilizer set at zero degrees, it is believed that alteration of the stabilizer setting would have a negligible effect upon the hinge moments within the practically useful range of flap angles as this is known to be true of an unbalanced flap.[7] The curves indicate that with either flap the hinge may safely be set back far enough to reduce the values of the hinge moments to small fractions of those corresponding to the unbalanced condition. It was decided to hinge the flap with the round leading edge at 0.25 flap chord and the other one at 0.30 flap chord; by this choice, approximately the same average value of the hinge moment is provided for the useful range of flap angles in each case.

The first tests of the balanced flaps were made with the servo of 1.8″×28.45″—see Fig. 5(c). That it proved powerful enough to displace either flap beyond the angle of maximum lift is shown by Figs. 13, 15 and 16. It is also of interest that the addition of the servo has similar effects upon the lift characteristics of each one, i.e., lift curve slopes are changed very slightly and the maxima are reduced about equally in both cases. This fact may be of value in future investigations of the balancing of surfaces which are intended to carry servo flaps.

When we compare the lift curves for the control surfaces which have balanced and unbalanced flaps (Figs. 14, 15 and 16), it becomes apparent that the effect of substituting servo for manual control is a serious limitation of maximum lift coefficient in the case of the unbalanced arrangement whereas very small effects of the same nature are experienced with balanced flaps.

The range and efficiency of control provided by the use of the same servo flap with the three forms of main flap are illustrated by Fig. 18. The control efficiency, $\eta$, is defined as $C_L$ (with servo)/$C_L$ (without servo) at equal flap angles. The differences between the efficiency and range of control available in the three cases are readily apparent. Viewed in this light, balancing of the main flap is obviously desirable and an elliptic leading edge is definitely superior to a round one.

The polar curves presented in Fig. 17 indicate that no important change of drag is associated with either the balancing of the control flap or the addition of the servo thereto; a very considerable increase of resistance occurs when a servo is added to the unbalanced flap, even though the maximum lift of this combination is relatively small.

## Servo *vs.* Manually Operated Control Surfaces

A discussion of the relative merits of servo operated *vs.* manually operated control surfaces for very large aircraft necessarily involves consideration of some questions not specifically treated in these experiments. The one of primary importance is: Can a very large control surface be so delicately balanced as to be easily operated and yet not be unstable under some conditions likely to occur in flight? British investigators seem to doubt that this can be accomplished.[8] The hinge moment tests previously described are not sufficiently complete to justify a broad conclusion but it seems safe to predict, for airplanes of the largest size now in existence, that adequate balance may be obtained by the use of an inset hinge and a suitable flap profile—if we do not demand that a pilot shall be able to deflect the flap to a position beyond that corresponding to maximum lift. In this connection, it is interesting to note that both the Sikorsky S-42 and the Dornier DoX have balanced control surfaces which are manually operated.

It would appear, therefore, that there is no urgent need for servo operated controls at present. It is conceivable, however, that heavier-than-air craft may continue to increase in size and that additional operating experience with very large airplanes may demonstrate that manually operated, balanced controls are not entirely satisfactory for such machines. In this eventuality, the servo operated control can be used to overcome the difficulty; for the present,

[7] Eastman N. Jacobs, and Robert M. Pinkerton, *Pressure Distribution over a Symmetrical Airfoil Section with Trailing Edge Flaps*, N.A.C.A. Technical Report No. 360, 1930.

[8] H. N. Garner, and C. E. W. Lockyer, *The Aerodynamics of a Simple Servo Rudder System*, Advisory Committee for Aeronautics (Great Britain), R. and M. No. 1105, 1927.

however, the servo flap will undoubtedly have trimming and balancing as its principal functions.

Before presenting formal conclusions, it may be worth while to point out that the results of these tests are equally applicable to the design of trimming flaps and servo controls.

## Conclusions

Although it appears that direct manual operation of the controls of any existing airplane may be rendered satisfactorily light by known methods of balancing, the servo control flap is of great potential value as a control operating or balancing device and as a means of maintaining trim without effort on the part of a pilot.

The substitution of servo for manual operation of an unbalanced control surface involves a serious limitation of maximum lift. For this reason, balancing of the main flap is recommended if a servo is to be used either as a trimmer or as a control operating device. The shape of the leading edge of a main flap with an inset hinge is important and an elliptical form is suggested for this part of the profile.

For a control surface which has fixed and movable portions of approximately equal size, a servo flap having an area equal to one-fifth that of the main flap is adequate as a control operating device and larger than is necessary for trimming.

Variation of the aspect ratio of the servo flap between the limits of five and fifteen is of negligible importance if the servo span be kept within 0.8 of the span of the control surface.

When a servo flap is attached to the trailing edge of a main control flap, it is of no advantage to hinge the servo about an axis aft of its own leading edge.

# The Drag of Tapered Cantilever Airfoils

R. H. UPSON AND M. J. THOMPSON, *Ann Arbor, Michigan*

(Received August 6, 1934)

A relatively simple empirical equation is set up to fit the experimental values of profile drag determined from N.A.C.A. tests on uniform-section rectangular airfoils of varying thickness, camber, etc., and at varying lift coefficients. This is made the basis for determining the profile drag of the more general airfoil whose chord and section vary along its span, and specifically the practical case of straight taper in planform and thickness ratio. The recognized theoretical expression for induced drag is similarly put into more useable form, and combined with the profile drag to get the following complete expression for the drag coefficient of a tapered airfoil:

$$C_D=[\text{R.N.}]_m^{-0.15}(0.0065\varphi+0.125\psi t_0^2)(1+0.7C_L^3)+0.318C_L^2(S/b^2+\gamma)$$

where $[\text{R.N.}]_m$ is the Reynolds number based on the mean geometric chord; $t_0$ is the root thickness ratio; $b^2/S$ is the aspect ratio; and $\varphi$, $\psi$ and $\gamma$ are mathematical functions of the taper characteristics which have been put into convenient tabular and chart form. After showing that the equation checks closely with known experimental results for tapered airfoils, up to near the stall, numerical computation is extended to a series of cantilever airfoils, varying in taper characteristics, but related to each other on an assumed basis of structural equivalence. Interesting conclusions of practical importance are derived therefrom, showing particularly the value of tapering the planform almost to a point, the small importance of tapering the thickness ratio in such a case, and the comparatively large drag of the elliptical wing. It is incidentally brought out that the present criterion for the computation of wing bending moments is in error on the unsafe side for highly tapered wings; and an improved formula for lateral center of pressure is established, its distance from the wing root being given by: $\bar{x}_p=b(0.185+0.085K_y-0.020K_y^2)$ for straight tapered wings without twist; where $b$ is the span, and $K_y$ is the ratio of tip chord to root chord.

---

AT the present time there is a sufficient mass of wind tunnel data available on the drag of airfoils of rectangular planform so that it is possible to compute quite accurately the resistance of such wings at angles of attack below the burble point.[1] In the case of tapered wings, however, an estimation of the drag is considerably more difficult. There is no satisfactory method for the determination of the profile drag which takes into account all of the factors involved, while the theoretical methods developed by Glauert[2] for the calculation of the induced drag of tapered wings are quite unsuited to engineering use.

The present paper is concerned with the development of a method whereby the complete drag coefficient for a wing of any arbitrary taper in planform and in thickness, aspect ratio, and root thickness ratio is determined as a function of the Reynolds number based on the mean geometric chord. The results are applied to the calculation of several tapered wings for which experimental data are available and excellent agreement is found between the wind tunnel tests and the computed values.

The method also lends itself readily to a consideration of the relative merits of the tapered wing as compared with other planforms from a combined aerodynamical and structural standpoint. Such an analysis is carried out and the superiority of highly tapered wings in this regard is definitely shown.

## 1. CALCULATION OF PROFILE DRAG

The basic assumption made in the present method for the calculation of the profile drag of a tapered wing is that the wing may be divided into a series of elementary chordwise strips each of which acts independently of the others. The drag of the entire wing may then be obtained by integration from test results on its component sections. Such a process is greatly facilitated by a simple empirical equation connecting the essential variables.

The first step is the determination of an expression for the profile drag coefficient of an elementary section of the wing. Making use of

[1] G. J. Higgins, *The Prediction of Airfoil Characteristics*, N.A.C.A. T.R. No. 312 (1929).

[2] H. Glauert, *Aerofoil and Airscrew Theory* (1926), Chapter XI.

the large mass of data[3] now available from the Variable Density Wind Tunnel of the National Advisory Committee for Aeronautics, at Reynolds numbers of approximately 3,000,000, the following equation will be found to fit the family of symmetrical airfoils of varying thickness ratio $t$. At zero lift the minimum profile drag coefficient may be written in the form

$$C_{D_0\,\text{min.}} = a_1 + a_2 t^2. \tag{1}$$

With $a_1 = 0.0065$, $a_2 = 0.125$, this matches the observed points within the limits of experimental error, fits the condition $t = 0$ better than the similar equation suggested in reference 3, and by having one less term is more easily handled.

It should be mentioned here that the tests on which this formula is based are subject to several errors[4] so that the values of $a_1$ and $a_2$ may be subject to future modification when more accurate test data are available. For this reason the analysis has been carried out using the algebraic coefficients in Eq. (1), and the numerical values are then introduced in the final results.

For a given value of $C_L$, Eq. (1) may be modified empirically so as to read

$$C_{D_0} = (a_1 + a_2 t^2)(1 + a_3 C_L^3). \tag{2}$$

This expression represents approximately the envelope of the curves of $C_{D_0}$ against $C_L$ for airfoils of varying camber in the range below the stall. For the data given in reference 3, $a_3$ has the value 0.7. The introduction of the term in $C_L^3$ in Eq. (2) is not entirely rational since for negative lifts the drag would decrease instead of increase. However, the expression agrees very well with observed data and its use may therefore be justified on an empirical basis as long as we restrict ourselves to positive values of $C_L$.

In the case of a tapered wing, consideration must be given to the fact that the chord may decrease markedly from root to tip and that there may consequently be an appreciable change in the Reynolds number of the elementary wing strips of very highly tapered wings. It will now be assumed that the drag coefficient is related to the Reynolds number, R. N., by the exponential law

$$C_{D_0} = h[\text{R.N.}]^n f(t,\, C_L). \tag{3}$$

This expression is not entirely satisfactory except for a flat plate set at zero angle of attack in which case the drag is pure skin friction. For the high Reynolds numbers considered in this work, the boundary layer is undoubtedly almost completely turbulent and $n$ has the value of $-1/5$ based on the assumption of a boundary layer velocity distribution which varies as the 1/7th power of the distance from the plate. Kármán,[5] however, has pointed out that as the Reynolds number increases the exponent 1/7 of the velocity distribution becomes smaller and smaller with a consequent change in the value of $n$. He has derived a logarithmic law for skin friction which is undoubtedly more exact than the exponential one but which is much too complicated to be used in this problem.

A more serious problem lies in the determination of the scale effect on the form drag for airfoils of finite thickness and camber. At present no satisfactory theory is available for the calculation of this effect and we are therefore again compelled to resort to empirical methods. Although such experimental data as exist are rather meager and incomplete, fairly satisfactory agreement with wind tunnel tests is obtained if Eq. (3) is used for the entire profile drag coefficient and $n$ is put equal to $-0.15$.

The profile drag coefficient of any element of the wing may thus be written as

$$C_{D_0} = h[\text{R.N.}]^n (a_1 + a_2 t^2)(1 + a_3 C_L^3), \tag{4}$$

where $\text{R.N.} = Vy/\nu = \rho Vy/\mu$, $y$ being the chord of the section, $V$ the velocity of flight, $\nu$ the kinematic coefficient of viscosity, $\rho$ the mass density of the air, and $\mu$ its absolute viscosity coefficient. At the standard temperature of 60°F, $\mu$ has the value $3.78 \times 10^{-7}$. The value of $h$ is determined by the fact that if $[\text{R.N.}]_e$ is the Reynolds number of the experiments on which

[3] Jacobs, Ward and Pinkerton, *The Characteristics of Seventy-Eight Related Airfoil Sections from Tests in the Variable Density Wind Tunnel*, N.A.C.A. T.R. No. 460 (1933).

[4] Reference 3, pp. 45–46.

[5] Th. von Kármán, *Turbulence and Skin Friction*, J. Aero. Sci. **1**, 1 (1934).

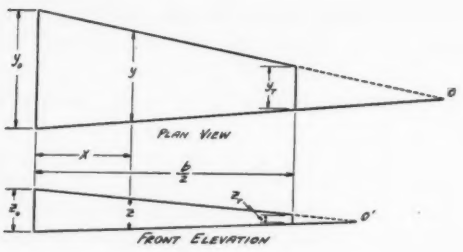


FIG. 1. Tapered wing diagram.

the values of $a_1$, $a_2$ and $a_3$ are based, then $h[\text{R.N.}]_e{}^n=1$.

We are now prepared to take up the calculation of the profile drag of the tapered wing. Practical considerations usually demand a straight taper from the longitudinal axis out to near each tip. If $t$ varies from root to tip, the same requirement for straight elements usually applies, but this does not mean that $t$ itself varies uniformly. Referring to Fig. 1, let $z$ be the maximum thickness and $y$ the chord of any given section at a distance $x$ from the root. Then locally the thickness ratio is $t=z/y$. If the wing elements focus at 0 in plan view, then in general they will focus at 0′ in front elevation if $t$ is to be other than uniform. Neglecting any change of shape or rounding off at the tip, let

$$K_y=y_T/y_0;\ K_z=z_T/z_0;\ K_t=t_T/t_0=K_z/K_y, \quad (5)$$

where the subscripts $T$ and 0 designate the tip and root, respectively. If $b$ is the total span, then

$$y=y_0\left[1-\frac{2x(1-K_y)}{b}\right];$$

$$z=z_0\left[1-\frac{2x(1-K_z)}{b}\right] \quad (6)$$

and

$$t=t_0\left[\frac{b-2x(1-K_z)}{b-2x(1-K_y)}\right].$$

The drag coefficient for any section of the wing is obtained from Eq. (4), so that considering only the case of no aerodynamic twist, or in other words, a constant lift coefficient along the span, we get for the profile drag of the entire wing

$$D_0=h(1+a_3C_L{}^3)q\int_{-b/2}^{b/2}(a_1+a_2t^2)\left(\frac{Vy}{\nu}\right)^n y\,dx$$

$$=2hqy_0\left(\frac{Vy_0}{\nu}\right)^n(1+a_3C_L{}^3)\int_0^{b/2}\left[a_1+a_2t_0{}^2\left\{\frac{b-2x(1-K_z)}{b-2x(1-K_y)}\right\}^2\right]\left[1-\frac{2x(1-K_y)}{b}\right]^{n+1}dx,$$

where $q=\rho V^2/2$ is the dynamic pressure. The profile drag coefficient for the entire wing is $C_{D_0}=D_0/qS$, where the wing area is $S=(y_0b/2)\times(1+K_y)$. We shall also find it most convenient to introduce the Reynolds number referred to the mean geometric chord, this latter quantity being $y_m=y_0(1+K_y)/2$. After carrying out the integration we finally obtain

$$C_{D_0}=[\text{R.N.}]_m{}^n(\varphi a_1+\psi a_2t_0{}^2)(1+a_3C_L{}^3), \quad (7)$$

where $[\text{R.N.}]_m=Vy_m/\nu$,

$$\varphi=\frac{2^{n+1}h(1-K_y{}^{n+2})}{(n+2)(1+K_y)^{n+1}(1-K_y)},$$

$$\psi=\frac{1}{(1+K_y)^{n+1}(1-K_y)}\times\left[\psi_1-\left(1-\frac{1-K_z}{1-K_y}\right)(\psi_2-\psi_3)\right]$$

and

$$\psi_1=\frac{2^{n+1}h(1-K_y{}^{n+2})}{n+2}\left(\frac{1-K_z}{1-K_y}\right)^2,$$

$$\psi_2=\frac{-2^{n+1}h(1-K_y{}^n)}{n}\left(1-\frac{1-K_z}{1-K_y}\right),$$

$$\psi_3=\frac{2^{n+2}h(1-K_y{}^{n+1})}{n+1}\left(\frac{1-K_z}{1-K_y}\right).$$

It will be noted at once that both functions $\varphi$ and $\psi$ become indeterminate as $K_y$ approaches unity, corresponding to the rectangular wing. The limiting value of $\varphi$ is easily found by

differentiation to be Lim $\varphi=h$; $K_y\to 1$. In order to find the limiting value of $\psi$, we put $K_y=1-\lambda$ and expand in a power series in $\lambda$. We get after simplification

$$\psi=\frac{2^{n+1}h}{(2-\lambda)^{n+1}}\left[\frac{(1-K_z)^2}{3}\left\{1-\frac{3c_1\lambda}{4}+\frac{3c_2\lambda^2}{10}-\frac{c_3\lambda^3}{12}+\frac{c_4\lambda^4}{56}\cdots\right\}\right.$$
$$\left.-(1-K_z)\left\{1-\frac{2c_1\lambda}{3}+\frac{c_2\lambda^2}{4}-\frac{c_3\lambda^3}{15}+\frac{c_4\lambda^4}{72}\cdots\right\}+\left\{1-\frac{c_1\lambda}{2}+\frac{c_2\lambda^2}{6}-\frac{c_3\lambda^3}{24}+\frac{c_4\lambda^4}{120}\cdots\right\}\right], \tag{8}$$

where $c_1=n-1$,
$c_2=(n-1)(n-2)$,
$c_3=(n-1)(n-2)(n-3)$,
$c_4=(n-1)(n-2)(n-3)(n-4)$,

so that

$$\lim_{\lambda\to 0}\psi=h[(1-K_z)^2/3-(1-K_z)+1]$$
$$=(h/3)(1+K_z+K_z^2),$$

which agrees with what would be obtained directly for the rectangular wing.

For the data considered in this paper we have, as mentioned on page 169, $a_1=0.0065$, $a_2=0.125$, $a_3=0.7$ when $R_c=3{,}000{,}000$, so that $h=9.366$ while we shall take $n=-0.15$. The corresponding values of $\varphi$ and $\psi$ for various values of $K_y$ and $K_z$ are given in Table I and are plotted in Fig. 2. In determining the values of $\psi$, it was found that in order to get satisfactory results when using the expression (7) it was necessary to carry through the computations with a large number of significant figures for values of $K_y$ near unity. For this reason the expansion in terms of $\lambda$ given in (8) was used for the range $0.7\leqslant K_y\leqslant 1$ while the exact formula (7) was used for $0\leqslant K_y\leqslant 0.7$. For $K_y=0.7$ the two formulas give results in entirely satisfactory agreement.

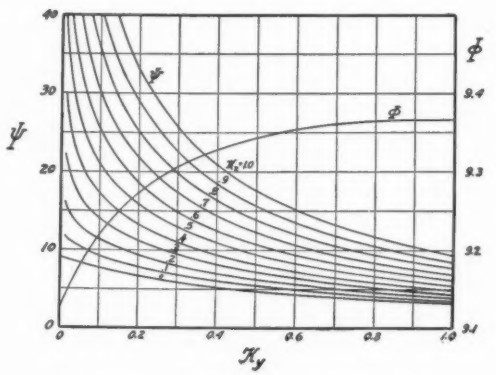


FIG. 2. Values of $\Psi$ and $\Phi$ for calculation of $C_{D_0}$.

It will be noted that as $K_y$ approaches zero, the value of $\psi$ becomes infinite (except for $K_z=0$). These cases, of course, are of no practical significance since they correspond to wings having full taper in planform but only partial taper in thickness. The wing element at the tip thus becomes a section of infinite thickness ratio, and according to our original assumption its profile drag is infinite. Obviously this analysis does not apply to such extreme cases, since Eq. (1) is valid only for thickness ratios up to about 35 percent.

It should also be mentioned that this analysis gives the true minimum profile drag only for symmetrical sections, but it is a very close approximation for all good sections of small camber. In any case, it is a more fundamental representation of the effect of thickness variations than to deal with the actual minimum drag of cambered sections. The latter are more properly dealt with through the medium of lift coefficient as has been done here.

It is thus apparent that the mean effective thickness ratio of a straight-tapered wing is not a simple arithmetic mean, nor yet the value corresponding to the position of the so-called mean aerodynamic chord employed in center of pressure relations. The latter is the chord through the lateral centroid of area corresponding to

$$\bar{x}=b(1+2K_y)/6(1+K_y), \tag{9}$$

whereas the position of the section with mean effective thickness ratio could be obtained approximately (since $\varphi$ is practically constant) by putting $t=t_0(\psi)^{\frac{1}{2}}$ and solving for $x$, a totally useless procedure in this case.

TABLE I. *Values of $\varphi$ and $\psi$ for calculation of basic profile drag coefficient of tapered wings.*

| | $\varphi$ | $\psi$ | | | | | | | | | | |
|---|---|---|---|---|---|---|---|---|---|---|---|---|
| $K_y$ | | $K_z=0$ | 0.1 | 0.2 | 0.3 | 0.4 | 0.5 | 0.6 | 0.7 | 0.8 | 0.9 | 1.0 |
| 0 | 9.13 | 9.13 | ∞ | ∞ | ∞ | ∞ | ∞ | ∞ | ∞ | ∞ | ∞ | ∞ |
| 0.01 | | 8.94 | 11.70 | 16.13 | 22.22 | 29.99 | 39.43 | 50.55 | 63.33 | 77.77 | 93.89 | 111.67 |
| 0.02 | | 8.76 | 11.20 | 14.70 | 19.88 | 26.13 | 33.64 | 42.42 | 52.48 | 63.80 | 76.40 | 90.26 |
| 0.04 | | 8.45 | 10.53 | 13.52 | 17.43 | 22.25 | 27.98 | 34.63 | 42.20 | 50.68 | 60.06 | 75.09 |
| 0.06 | | 8.16 | 10.02 | 12.61 | 15.94 | 20.01 | 24.81 | 30.34 | 36.61 | 43.61 | 51.35 | 59.83 |
| 0.08 | | 7.90 | 9.59 | 11.91 | 14.84 | 18.40 | 22.58 | 27.38 | 32.80 | 38.84 | 45.50 | 52.78 |
| 0.10 | 9.22 | 7.62 | 9.22 | 11.30 | 13.96 | 17.14 | 20.86 | 25.13 | 29.93 | 35.27 | 41.15 | 47.57 |
| 0.20 | 9.27 | 6.64 | 7.79 | 9.27 | 11.08 | 13.22 | 15.68 | 18.47 | 21.59 | 25.04 | 28.81 | 32.91 |
| 0.30 | 9.31 | 5.84 | 6.78 | 7.92 | 9.31 | 10.92 | 12.76 | 14.84 | 17.14 | 19.69 | 22.45 | 25.46 |
| 0.40 | 9.33 | 5.24 | 6.00 | 6.93 | 8.04 | 9.33 | 10.79 | 12.43 | 14.25 | 16.24 | 18.41 | 20.76 |
| 0.50 | 9.34 | 4.73 | 5.37 | 6.15 | 7.08 | 8.14 | 9.34 | 10.69 | 12.17 | 13.80 | 15.57 | 17.47 |
| 0.60 | 9.35 | 4.31 | 4.86 | 5.53 | 6.31 | 7.21 | 8.22 | 9.35 | 10.60 | 11.96 | 13.44 | 15.03 |
| 0.70 | 9.36 | 3.94 | 4.51 | 5.00 | 5.68 | 6.45 | 7.33 | 8.30 | 9.36 | 10.52 | 11.78 | 13.13 |
| 0.80 | 9.36 | 3.63 | 4.06 | 4.57 | 5.16 | 5.84 | 6.59 | 7.44 | 8.36 | 9.36 | 10.45 | 11.62 |
| 0.90 | 9.37 | 3.35 | 3.74 | 4.20 | 4.74 | 5.32 | 5.98 | 6.72 | 7.53 | 8.40 | 9.37 | 10.39 |
| 1.00 | 9.37 | 3.12 | 3.47 | 3.87 | 4.34 | 4.87 | 5.46 | 6.12 | 6.84 | 7.62 | 8.46 | 9.37 |

$K_y$ = tip chord/root chord; $K_z$ = tip thickness/root thickness.

## 2. CALCULATION OF THE INDUCED DRAG

It is well known that the induced drag coefficient of any wing may be written in the form

$$C_{D_i}=(C_L^2S/\pi b^2)(1+\delta), \tag{10}$$

where $\delta$ is dependent on the shape of the planform and is zero for an elliptical wing. The value of $\delta$ for the rectangular wing has been determined by Glauert[6] as a function of the aspect ratio, while similar calculations have also been carried out for wings of any arbitrary taper in planform, but for only one aspect ratio, its value being equal to $\beta$, the lift curve slope for infinite aspect ratio. Now the angle of attack for the finite aspect ratio wing is, when measured in radians,

$$\alpha=\alpha_\infty+(C_LS/\pi b^2)(1+\tau),$$

where $\tau$, like $\delta$, is dependent on the planform shape. Differentiating with respect to $C_L$, we obtain for the lift curve slope

$$\frac{dC_L}{d\alpha}=\frac{\beta}{1+(\beta/\pi)(S/b^2)(1+\tau)}.$$

If the value of 0.072 is considered as an average value of $dC_L/d\alpha$ for rectangular wings of aspect ratio 6, when the angle of attack is measured in degrees, then the above formula may be used to determine a suitable value for $\beta$. In this case we find, using Glauert's value for $\tau$, that $\beta=5.56$ ($\alpha$ in radians), or 0.097 ($\alpha$ in degrees).

The method employed by Glauert for the determination of the values of $\delta$ may, of course, be applied to tapered wings of any aspect ratio. The process as outlined in reference 2 finally reduces to the solution of a system of four linear equations in four unknowns, and in the general case of a wing of any taper and aspect ratio these equations would have algebraic coefficients. Even in particular cases where the coefficients may be reduced to numerical quantities, the process is a long and tedious one and for this reason we have adopted an approximate method of treating this phase of the problem.

In the case of the rectangular wing the value of $\delta$ considered as a function of aspect ratio may be represented approximately by the empirical equation

$$\delta=0.049(b^2/S)/\beta=0.00881b^2/S. \tag{11}$$

The agreement with the computed values of $\delta$ could undoubtedly be improved by the use of a second degree equation but if it is remembered that $\delta$ always enters into the expression for the induced drag coefficient in the form $1+\delta$ and is usually small, it is seen at once that an error in the value of $\delta$ will produce only about one-tenth of that error in $C_{D_i}$. The above simplification thus appears to be entirely justified and Eq. (11) will be found satisfactory for aspect ratios from 4 to 16.

Now for the tapered wing of aspect ratio equal to $\beta$, the value of $\delta$ as a function of $K_y$, the planform taper, is empirically

$$\delta=0.141-0.404(K_y)^{\frac{1}{2}}+0.311K_y. \tag{12}$$

For tapered wings of any other aspect ratio, we shall assume that $\delta$ is affected by changes in aspect ratio alone in exactly the same way as

[6] H. Glauert, reference 2, ¶ 11.4–11.5.

the rectangular wing. Thus we may combine Eqs. (11) and (12) and write as an approximate general expression

$$\delta = K(b^2/S)(0.141 - 0.404K_y^{\frac{1}{2}} + 0.311K_y).$$

The constant $K$ is determined by the condition that when $b^2/S = \beta$, $K(b^2/S) = 1$, so that we finally obtain

$$\delta = (b^2/S)(0.0254 - 0.0727K_y^{\frac{1}{2}} + 0.0560K_y). \quad (13)$$

The expression for the induced drag coefficient is now found to be

$$C_{D_i} = (C_L^2/\pi)(S/b^2 + \gamma), \quad (14)$$

where $\gamma = 0.0254 - 0.0727(K_y)^{\frac{1}{2}} + 0.0560K_y$. (See Table IV for numerical values.)

On inspection of Eq. (14), it is evident that a small part of the so-called induced drag coefficient has little or no dependence on aspect ratio but is exclusively a function of lift coefficient. The same applies to an important part of the so-called profile drag given by Eq. (7), except for the slight Reynolds number effect. The latter, as already pointed out, is of doubtful justification in the form used except for that portion of the drag directly due to skin friction. Hence there is no basic reason, beyond that of arbitrary definition, for classifying such parts of the drag as either profile or induced. But in view of the general acceptance of Glauert's values, approximately represented by Eq. (14), as "induced drag," we arbitrarily call the entire balance "profile drag" and choose our empirical equation to correspond. This was the classification assumed in working up all the results from reference 3 and should be kept in mind in the interpretation of other experimental data.

### 3. Comparison with Experimental Results

The complete drag coefficient for tapered airfoils may now be written as

$$C_D = [\text{R.N.}]_m^n(\varphi a_1 + \psi a_2 t_0^2)(1 + a_3 C_L^3) + (C_L^2/\pi)(S/b^2 + \gamma),$$

where $\varphi$, $\psi$ and $\gamma$ are obtained from Eqs. (7) and (14). Using the previously mentioned numerical values for the various constants (see page 171) we obtain

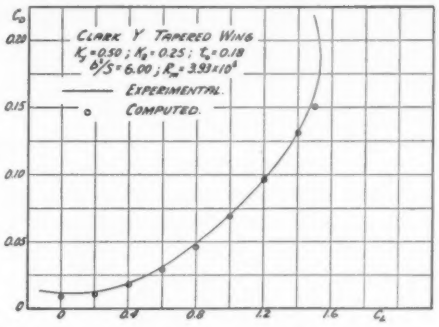


FIG. 3. Experimental and computed drag coefficients for tapered airfoils.

$$C_D = [\text{R.N.}]_m^{-0.15}(0.0065\varphi + 0.125\psi t_0^2) \times (1 + 0.7C_L^3) + (C_L^2/\pi)(S/b^2 + \gamma). \quad (15)$$

In order to check the accuracy of the various assumptions on which our theory is based, computations have been carried out for several tapered wings for which experimental data exist. The results for the tapered Clark $Y$ wing[7] are shown in Fig. 3 and the agreement is found to be quite satisfactory except at and beyond the neighborhood of maximum lift. Comparisons with other tests in the variable density tunnel, including the case of a tapered wing with rectangular center section,[8] show equally good agreement, but in the case of tests at low Reynolds numbers in atmospheric tunnels, such factors as turbulence would undoubtedly require a modification of the coefficients in the basic profile drag equation, and possibly a change in the exponent of the Reynolds number.

In connection with the expression for the complete drag coefficient given in Eq. (15), it should be noted that the quantities $[\text{R.N.}]_m^{-0.15}$ and $\varphi$ are almost constant for the usual conditions encountered in practice. Thus when the taper factors are once determined so as to give an optimum value of $\psi$, this equation is very appreciably simplified and readily lends itself to a further study of the effect of variations in design characteristics.

---

[7] R. F. Anderson, *The Aerodynamic Characteristics of Three Tapered Airfoils Tested in the Variable Density Wind Tunnel*, N.A.C.A. T.N. No. 367 (1931).

[8] R. F. Anderson, *Tests of Three Tapered Airfoils Based on the N.A.C.A. 2200, the N.A.C.A.-M6, and the Clark Y Sections*, N.A.C.A. T.N. No. 487 (1934).

## 4. Relative Merit of Various Planforms

From a purely aerodynamic point of view, the ideal wing would be one which for a given aspect ratio gave minimum values of $\varphi$, $\psi$ and $\gamma$. A practical comparison of different airfoils must, however, include consideration of certain structural factors. If we assume full depth wing beams in various cantilever wings, each carrying a concentrated load $W$ at mid-span to balance the distributed lift, the root bending moment must be

$$M_0=(W/2)\bar{x}_p, \tag{16}$$

where $\bar{x}_p$ is the lateral center of pressure distance from mid-span. The U. S. Department of Commerce requirements, in effect, make $\bar{x}_p$ equivalent to $\bar{x}$ in Eq. (9), subject to allowance for the width of the fuselage. Though this is a safe assumption for most wings hitherto in use, it is open to serious question for the highly tapered wings, as will now be apparent.

An exact expression for $M_0$ may be found for a tapered wing using the aerodynamic theory which forms the basis for induced drag calculations.[9] According to Glauert's work given in reference 2, the spanwise distribution of circulation along the wing may be represented approximately by the first four terms of a Fourier's series; that is,

$$\Gamma=2bV(A_1\sin\theta+A_3\sin 3\theta+A_5\sin 5\theta+A_7\sin 7\theta),$$

where $x=-(b/2)\cos\theta$ and the coefficients $A_1 \cdots A_7$ depend on the shape of the planform and the aspect ratio. We now assume that the Kutta-Joukovsky theorem holds for each elementary wing strip, so that $dL=\rho V\Gamma dx$ and the total lift is readily found to be

$$L=\pi\rho V^2b^2A_1/2. \tag{17}$$

In a similar way we may calculate the bending moment at the root section. We have

$$M_0=\int_0^{b/2}xdL$$

$$=(\rho b^3V^2/2)(A_1/3+A_3/5-A_5/21+A_7/45),$$

or introducing the lift from (17) and putting it equal to the total load $W$, we get

$$M_0=(Wb/\pi A_1)(A_1/3+A_3/5-A_5/21+A_7/45),$$

so that

$$\bar{x}_p=(2b/\pi)(\tfrac{1}{3}+A_3/5A_1-A_5/21A_1+A_7/45A_1). \tag{18}$$

The values of the ratios $A_3/A_1$, $A_5/A_1$, etc., are readily calculated from the tables given in reference 2. The values of $\bar{x}_p/b$ for rectangular wings of different aspect ratios are given in Table II.

Table II. *Lateral center of pressure position vs. aspect ratio for rectangular wings.*

| $(b^2/S)/\beta$ | $(b^2/S)(\beta=5.56)$ | $\bar{x}_p/b$ |
|---|---|---|
| 0.50 | 2.78 | 0.2225 |
| 0.75 | 4.17 | 0.2250 |
| 1.00 | 5.56 | 0.2275 |
| 1.25 | 6.95 | 0.2290 |
| 1.50 | 8.34 | 0.2310 |
| 1.75 | 9.73 | 0.2320 |

It thus appears that $\bar{x}_p$ is practically independent of aspect ratio and in the remainder of this work, such an assumption will be made.

For the tapered wing of aspect ratio $b^2/S=\beta$ Glauert's values of $A_1$, $A_3\cdots$ etc., may be used to calculate $\bar{x}_p/b$ for different values of $K_y$. The results are given in Table III.

Table III. *Lateral center of pressure position vs. planform taper for monoplane wing.*

| $K_y$ | $\bar{x}_p/b$ | $\bar{x}/b$ |
|---|---|---|
| 0 | 0.1843 | 0.1667 |
| 0.25 | 0.2045 | 0.2000 |
| 0.50 | 0.2145 | 0.2222 |
| 0.75 | 0.2220 | 0.2380 |
| 1.00 | 0.2275 | 0.2500 |

The values of $\bar{x}/b$ calculated from Eq. (9) are also given in Table III, and the results are plotted graphically in Fig. 4 as $2\bar{x}_p/b$, the lateral center of pressure position.

From the obvious fact that the force distribution in the general case differs from the area distribution along the span, our original assumption of zero aerodynamic twist must now be called into question even for geometrically untwisted airfoils. To take the extreme case of

[9] Similar calculations including both torsion and bending have been carried out with a somewhat different point of view by E. Amstutz, *Calculation of Tapered Monoplane Wings*, N.A.C.A. T.M. No. 578.

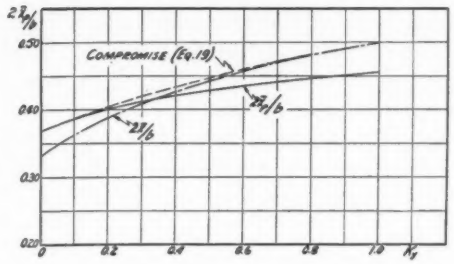


FIG. 4. Lateral center of pressure position *vs.* planform taper.

taper to a point, the local lift coefficient at $b/20$ from the tip is approximately 1.5 times the mean. The area to which this applies, however, is small; and at small values of $C_L$ the effect on the profile drag is small; while at large values of $C_L$ we must consider the three-dimensional flow and resultant burbling characteristics, which as yet are imperfectly known. Hence for profile drag purposes we shall continue to assume zero aerodynamic twist, which is equivalent to using an arithmetical mean of the lift coefficients. This can readily be shown to involve a negligible error in profile drag for a twist of any kind not exceeding about 5 degrees, except for the burbled condition above mentioned. The induced drag and lateral center of pressure for twisted airfoils can be taken from reference 2.

Returning now to the airfoil without twist, i.e., chord lines all parallel, and median camber proportional to chord, it will be noted that the geometric and aerodynamic curves in Fig. 4 cross each other at $K_y=0.34$, approximately. For larger values of $K_y$, i.e., for planforms more nearly rectangular, the assumption of uniform pressure distribution, usually approximated at the burble point, is obviously the more severe case. The more pointed wings, however, show an intensification of pressure at the tips, which is more severe for the unburbled flow, and just opposite to the commonly assumed "tip loss." We shall therefore take a compromise curve of

$$\bar{x}_p=b(0.185+0.085K_y-0.020K_y^2). \quad (19)$$

This single equation gives a good engineering approximation to the worst conditions of the other two curves, and is certainly simpler than Eq. (18).

Substituting (19) in (16) and dividing by $z_0$ we get the approximate root flange force $F$; then dividing by $W/2$, and expressing the result in terms of aspect ratio and root thickness ratio $t_0$, we finally obtain a so-called structural quotient,

$$Q_s=(b^2/2St_0)(1+K_y)(0.185+0.085K_y-0.020K_y^2). \quad (20)$$

For the rectangular wing, $K_y=1$ and this expression reduces to $Q_s=b^2/4St_0$, while for the elliptical wing, the aerodynamic theory gives $A_3=A_5=A_7=0$, so that $\bar{x}_p=2b/3\pi$, which is identical with the value for the lateral centroid of area. Thus the structural quotient for the elliptic wing becomes $Q_s=b^2/6St_0$.

A given value of the structural quotient approximately establishes the root force in the spar flange as a proportion of the gross load carried, and seems a logical basis of comparison for cantilever wings, particularly when of constant span.

It will be of interest now to compare characteristics of a series of wings on the rather liberal structural basis of $Q_s=5$ and aspect ratio $b^2/S=6$. Using the relations already laid down, we get the values shown in Table IV.

The wing proportions in the table have been arbitrarily chosen so as not to bring $t$ below 0.10 which is assumed as the structural minimum for torque stiffness. Below that point the saving in drag is small and is usually overbalanced by a more-than-proportional falling off of maximum lift.

It will be noted from Eq. (15) that an increase in $\gamma$ is exactly equivalent to a corresponding decrease in the reciprocal of the aspect ratio. Hence the latter can be used as a means of reducing the induced drag of all the airfoils to a common value. If the elliptical airfoil is arbitrarily chosen as the basis, each of the others can be brought into line by altering its $b^2/S$ factor, and finding the new value of $t_0$ which fits Eq. (20). $C'_{D_0}$ in the next to last column of Table IV is computed on this basis and thus forms a direct comparison of over-all merit from a drag standpoint.

TABLE IV. *Cantilever airfoil characteristics for equal root forces and aspect ratio 6, Reynolds number 3,000,000 based on mean chord.*

| Type of wing | $K_y$ | $K_x$ | $\gamma$ | Root $l_0$ | Tip $l_T$ | $\frac{2\bar{x}_p}{b}$ | Profile $C_{D_0}$ | | | Induced $C_{D_i}$ | | | Total $C_D$ | | | —Revised— $\frac{b_1^2}{S}$ | $C'_{D_0}$ | Order of merit |
|---|---|---|---|---|---|---|---|---|---|---|---|---|---|---|---|---|---|---|
| | | | | | | | $C_L=0$ | $C_L=0.3$ | $C_L=0.6$ | $C_L=0.9$ | $C_L=0.3$ | $C_L=0.6$ | $C_L=0.9$ | $C_L=0.3$ | $C_L=0.6$ | $C_L=0.9$ | | | |
| Untapered | 1.00 | 1.00 | 0.00867 | 0.300 | 0.300 | 0.500 | 0.0178 | 0.0180 | 0.0204 | 0.0267 | 0.0050 | 0.0201 | 0.0452 | 0.0230 | 0.0405 | 0.0719 | 6.32 | 0.0190 | 10 |
| Tapered in thickness only | 1.00 | 0.333 | 0.00867 | .300 | .100 | .500 | .0119 | .0121 | .0137 | .0180 | .0050 | .0201 | .0452 | .0171 | .0338 | .0632 | 6.31 | .0123 | 9 |
| 2 : 1 planform | .50 | .50 | 0.00200 | .200 | .200 | .445 | .0115 | .0117 | .0132 | .0174 | .0048 | .0193 | .0434 | .0165 | .0325 | .0608 | 6.07 | .0116 | 8 |
| Same + taper in thickness ratio | .50 | .25 | 0.00200 | .200 | .100 | .445 | .0101 | .0103 | .0116 | .0152 | .0048 | .0193 | .0434 | .0151 | .0309 | .0586 | 6.07 | .0102 | 6 |
| 4 : 1 planform | .25 | .25 | 0.00300 | .154 | .154 | .411 | .0094 | .0096 | .0108 | .0142 | .0049 | .0194 | .0437 | .0145 | .0302 | .0579 | 6.11 | .0095 | 5 |
| Same + taper in thickness ratio | .25 | .162 | 0.00300 | .154 | .100 | .411 | .0089 | .0091 | .0103 | .0134 | .0049 | .0194 | .0437 | .0140 | .0297 | .0571 | 6.11 | .0090 | 4 |
| 8 : 1 planform | .125 | .125 | 0.00667 | .132 | .132 | .391 | .0086 | .0087 | .0098 | .0129 | .0050 | .0199 | .0447 | .0137 | .0297 | .0576 | 6.24 | .0088 | 3 |
| Same + taper in thickness ratio | .125 | .095 | 0.00667 | .132 | .100 | .391 | .0084 | .0085 | .0096 | .0126 | .0050 | .0199 | .0447 | .0135 | .0295 | .0573 | 6.24 | .0086 | 2 |
| Tapered to point | 0 | 0 | 0.0253 | .111 | .111 | .370 | .0079 | .0080 | .0091 | .0119 | .0055 | .0220 | .0495 | .0135 | .0311 | .0614 | 6.92 | .0084 | 1 |
| Elliptical with uniform thickness ratio | — | — | 0 | .200 | .200 | .424 | .0115 | .0117 | .0132 | .0174 | .0048 | .0191 | .0429 | .0165 | .0323 | .0603 | 6.00 | .0115 | 7 |

## 5. CONCLUSIONS

In spite of unconsidered factors, various conclusions as to tapered cantilever wings may be drawn from this table as follows:

A four to one planform taper with a uniform thickness ratio of 15.4 percent is structurally about as effective as an untapered wing of 30 percent thickness, and has about half the basic profile drag.

The further reduction in profile drag of a highly tapered wing, by superimposing a taper in thickness ratio, is comparatively slight. If, however, considerations of arrangement, vision or otherwise dictate a more moderate degree of planform taper, the benefits of taper in thickness ratio are more substantial (12 percent profile drag reduction for the wing with $K_y=0.5$), but the drag is greater than that obtained with more highly tapered planforms alone.

From a standpoint of performance alone, and without regard to construction economics, the elliptical planform is about equivalent to the two-to-one planform taper and decidedly inferior to a taper of four-to-one for the entire range of lift coefficient.

The taper to a point appears best of all in the final order of merit, though quantitatively the margin is small between this and the 8 : 1 taper. Also it is apparent that the larger span required to equalize the induced drag will increase the spar flange weight approximately in proportion to the span, for equal flange force' If the thickness is further increased to maintain constant flange weight, the revised drag of the pointed airfoil is increased to approximately 0.0086 while the increase in the corresponding drag of the 8 : 1 airfoil is unnoticeable in the results as already given. On the other hand, minor considerations of distributed spar force and torsional stiffness theoretically favor the more pointed airfoil. Thus, though the absolute optimum for a specific case would call for a finite tip section, still it seems probable that tapers at least as high as 8 : 1 will be found advantageous for racing and large transports.

These conclusions on the relative merits of the highly tapered wing are, of course, based on the assumption that no difficulties will be encountered in obtaining satisfactory control and other necessary features. As the use of a highly

tapered wing requires a large root chord, the problem of wing-fuselage interference may become acute, especially in the case of low wing monoplanes. Proper filleting at the wing root may solve this difficulty, but further experimental investigation is certainly required[10]. The same also applies to maximum lift.

Preliminary analysis of problems involving change in aspect ratio, load distribution, strut drag, etc., may be handled in a similar manner[11] by the use of Eq. (15), assuming smoothly curved airfoil sections in the general range of proportions covered in reference 3.

[10] The case of a wing with $K_y=0.682$ has been studied by A. L. Klein, *Effect of Fillets on Wing-Fuselage Interference*, Trans. A.S.M.E. **56**, No. 1 (1934).

[11] For the effect of these and other variations on a complete airplane, see R. H. Upson, *Wings—A Coordinated System of Basic Design*, S.A.E. Journal, January, 1930; the coefficients being subject to further refinement as indicated in the present paper.

# The Cooling of Finned Cylinders

ARNOLD E. BIERMANN AND BENJAMIN PINKEL, *National Advisory Committee for Aeronautics*

(Submitted June 16, 1934)

THE cooling of hot bodies by means of metal fins exposed to an air stream can be treated as two related problems, one involving the convection of heat from the fin surfaces by the air stream and the other involving the conduction of heat through the fins to the fin surfaces. The rate at which heat is conveyed from a surface by an air stream is usually expressed as a surface heat transfer coefficient $q$. Theoretical methods have been developed for calculating the surface heat transfer coefficients for simple surfaces over which the air flow is known.[1] For complex bodies, such as finned cylinders, the velocity field over the surface of the fins is extremely complicated, especially in the region at the rear half of the cylinder where the flow is vortical. For such bodies experimental methods must be used at present for determining the surface heat transfer coefficient. An investigation has been conducted by the National Advisory Committee for Aeronautics, as a part of a general research on the cooling of finned cylinders, to determine the value of $q$ for a variety of fin constructions and a range of air speeds.

The second problem—the conduction of the heat through the fins—is simpler and the associated differential equation permits of solution in terms of functions of the fin dimensions and the surface heat transfer coefficient. Solutions have been given by Harper and Brown[2] and Schmidt[3] for various types of fins.

## EXPERIMENTAL WORK

Tests were conducted in a 30-inch closed throat tunnel (Fig. 1) to determine the values of $q$ for a series of 18 cylinders provided with the tapered and rectangular fins shown in section in Fig. 2. The cylinders were machined from forgings of S.A.E. 1050 steel and had outside wall diameters of 4.66 inches and wall thicknesses of 0.08 inch. All fins had a tip radius of 0.02 inch.

The cylinders were electrically heated and were provided with guard rings at each end to eliminate heat flow through the ends and to aid in obtaining two-dimensional air flow over the test section. Cylinder-wall and fin temperatures were measured by means of 24 iron-constantan ther-

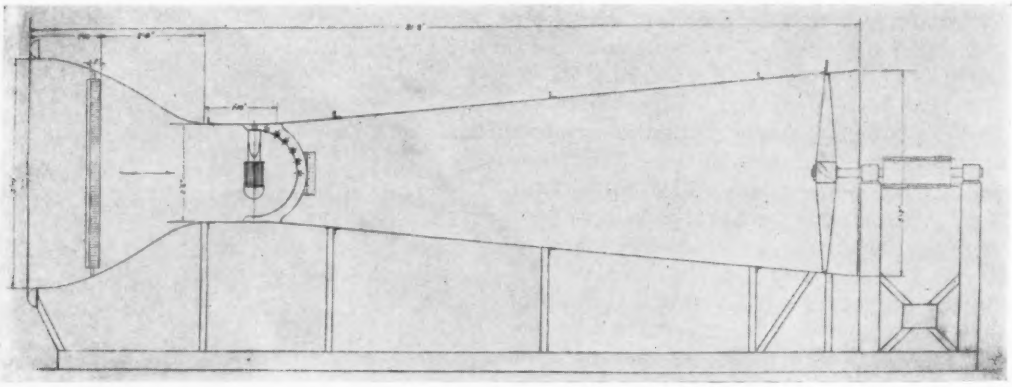

FIG. 1. Wind tunnel showing test unit mounted in place.

[1] A. Fage and V. M. Falkner, *Relation Between Heat Transfer and Surface Friction for Laminar Flow*, R. and M. No. 1408, British A.R.C., 1931.

[2] D. R. Harper, 3rd, and W. B. Brown, *Mathematical Equations for Heat Conduction in the Fins of Air-Cooled Engines*, Tech. Report No. 158, N.A.C.A., 1923.

[3] E. Schmidt, *Die Warmeubertragung durch Rippen*, V.D.I. Vol. 70, No. 26, June 26, 1926, pp. 885–889; and Vol. 70, No. 28, July 10, 1926, pp. 947–951.

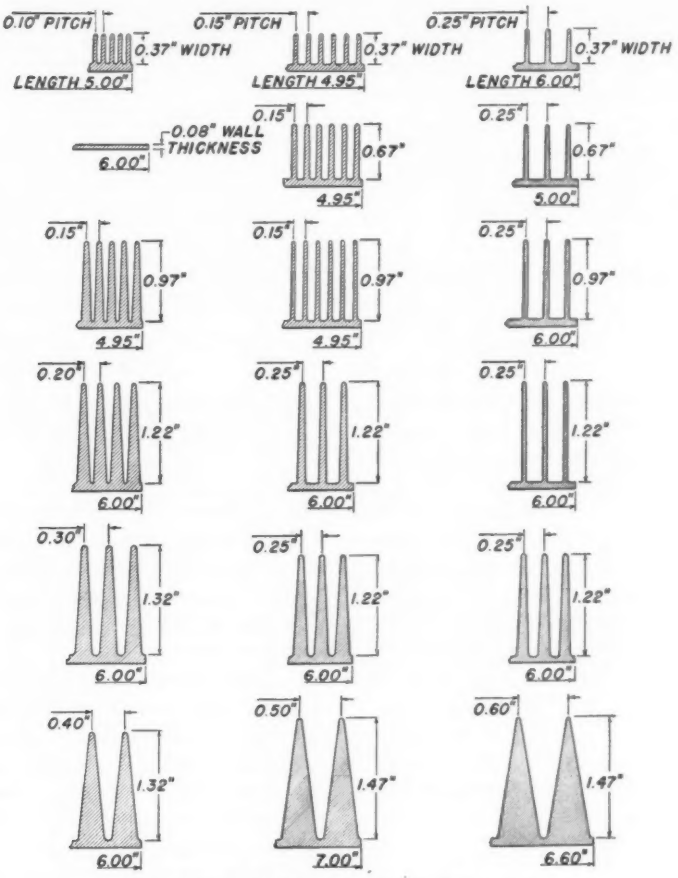


FIG. 2. Construction of finned cylinders tested.

mocouples, spot-welded to the cylinder wall and fins.

For each finned cylinder tested the average surface heat transfer coefficient was calculated by dividing the measured heat input by the product of the total cooling area and the average temperature difference between the total cooling surface and the cooling air.

A more detailed description of the test apparatus has been given in earlier publications.[4]

[4] Oscar W. Schey and Arnold E. Biermann, *Heat Dissipation from a Finned Cylinder at Different Fin-Plane Air-Stream Angles*, Tech. Report No. 429, N.A.C.A., 1932; Arnold E. Biermann and Benjamin Pinkel, *Heat Transfer from Finned Metal Cylinders in an Air Stream*, Tech. Report. N.A.C.A., 1934.

## SHAPE OF FINS

An extensive study of fin shapes has been made by Schmidt with the object of determining the profile of the lightest fin that will dissipate a required amount of heat for a given root temperature. Such fins are shown to be characterized by zero tip thickness and by having a linear temperature variation from the root to the tip, the tip temperature being that of the free air stream. For the simple case of a constant surface heat transfer coefficient over the entire fin the optimum profile was found to be composed of two congruent parabolas having their vertexes tangent to the median line at the fin tip. However, for the same cooling requirements the triangular fin was found to be only 4.5 percent

heavier. Since the tip must have a definite thickness, which for the thin fins used in modern air-cooled engines may be almost as great as the fin root thickness, the importance of determining the exact profile is lessened. From these considerations the tapered fin appears as the practical fin profile which best combines effective cooling with ease of manufacture.

## Surface Heat Transfer Coefficients

The problem of the transfer of heat from surfaces is closely related to skin friction and boundary-layer theory. The same mechanism that transmits momentum through a boundary layer also transmits heat. The heat transfer is greatest from those surfaces having a thin turbulent boundary layer of high average velocity.

For the case of potential flow about a cylinder the average velocity is highest at the cylinder surface and decreases to the velocity of the free air stream as the distance from the surface is increased. Actually, due to viscous effects, a boundary layer is built up on the surface of the cylinder causing the flow to break away from the cylinder at about 100° from the front to form a vortical wake at the rear of the cylinder. The flow is further modified by the presence of fins over the surfaces of which individual boundary layers are built up.

### Effect of fin width on $q$

Although the flow is considerably different from potential flow, the average velocity over narrow fins may still be expected to be greater than over wide fins, resulting in a higher surface heat transfer coefficient for the former case. The effect of fin width on $q$ is shown in Fig. 3 as determined from tests on finned cylinders having pitches of 0.15 inch and 0.25 inch. Increase in fin width up to about 0.40 inch results in an appreciable reduction in the value of $q$; whereas for a further increase in width the variation in the value of $q$ is much smaller. As most fins of practical interest have a width greater than 0.40 inch it may be assumed for purposes of calculation that $q$ is independent of fin width.

### Effect of fin space on $q$

For closely spaced fins the mutual interference of the boundary layers of adjacent fins restricts

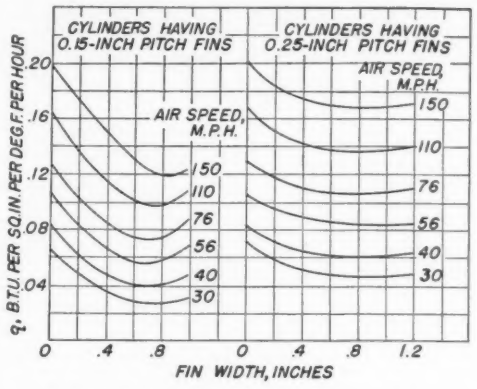


Fig. 3. Effect of varying the fin width on the average values of $q$ for cylinders having fins of 0.04-inch thickness and 0.15-inch and 0.25-inch pitch.

the air flow and results in a small surface heat transfer coefficient. As the fin spacing is increased the interference decreases and $q$ increases, until a point is reached where the flows over adjacent fins no longer interfere and $q$ approaches a limiting value.

Curves representing an average of all the surface heat transfer coefficients determined in the tests are shown in Fig. 4 plotted against the average air space $S$ between adjacent fins. These curves represent tests on rectangular and tapered fins of various thicknesses, widths, and taper angles. The average deviation of the test points from the curves is less than 8 percent, showing that the most important fin dimension governing the value of $q$ is $S$ and that the effect of variations in the other dimensions is small. For the range of spacings tested the value of $q$ varies with the 0.322 power of $S$.

### Effect of fin thickness on $q$

For a given value of $S$, variation in fin thickness does not have an appreciable effect on the air flow. Sufficient data were not collected to determine the independent effect of fin thickness. However, as previously pointed out in plotting Fig. 4, it was found that the thickness was of minor importance in determining the value of $q$.

### Variation of $q$ with velocity

From Fig. 4 the surface heat transfer coefficients were plotted against velocity on logarith-

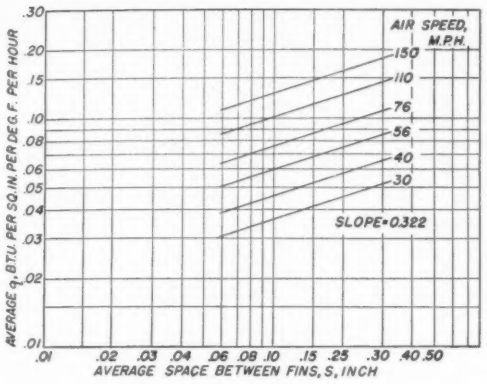


FIG. 4. Variation of average $q$ with the average fin space for all cylinders tested.

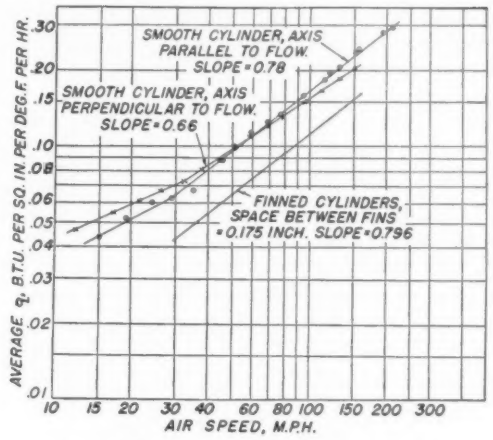
SMOOTH CYLINDER, AXIS PARALLEL TO FLOW. SLOPE=0.78
SMOOTH CYLINDER, AXIS PERPENDICULAR TO FLOW. SLOPE=0.66
FINNED CYLINDERS, SPACE BETWEEN FINS =0.175 INCH. SLOPE=0.796
AVERAGE q, B.T.U. PER SQ. IN. PER DEG. F. PER HR.
AIR SPEED, M.P.H.

FIG. 5. Effect of air speed on the surface heat transfer coefficient.

mic coordinates for a space of 0.175 inch (Fig. 5). The slope of the curve shows that the value of $q$ varies with the 0.796 power of the velocity. This exponent holds fairly well for the range of fin spacings tested. From theoretical considerations the value of $q$ for flat plates and tubes has been shown to vary with the 0.5 power of velocity for the case of laminar flow in the boundary layer and with the 0.8 power of velocity for the case of turbulent flow.

The effect of velocity on $q$ for a smooth cylinder tested with the axis both parallel and perpendicular to the air flow is also shown in Fig. 5. Each curve shows a transition point which for the case of the axis perpendicular to the flow occurs at a Reynolds number of 109,000. Fage[5] shows from tests on the drag of circular cylinders having their axes perpendicular to the air stream that a critical Reynolds number exists between 100,000 and 500,000, the higher the initial turbulence of the air stream the lower the critical Reynolds number.

**Effect of cylinder diameter and altitude on $q$**

The values of $q$ presented apply only to a cylinder diameter of 4.66 inches and an air density corresponding to sea-level conditions (29.92 inches of Hg and 80°F). The value of $q$ can be determined for other cylinder diameters and air densities by use of the theory of similitude. The important factors determining the value of $q$ are

$k_a$, thermal conductivity of the air
$\rho$, density of the air
$\mu$, viscosity of the air
$V$, velocity of the cooling air
$c_p$, specific heat of the cooling air

and the various dimensions determining the geometry of the body and its position relative to the air stream, which for the finned cylinder are

$D$, diameter of the cylinder
$S$, average air space between the fins
$t$, average thickness of the fins
$w$, width of the fins.

By dimensional analysis $q$ is expressed as a function of these quantities for a finned cylinder having its axis perpendicular to the air stream.

$$q = c_p \rho V f\left\{\left(\frac{\rho V D}{\mu}\right), \left(\frac{\mu c_p}{k_a}\right), \left(\frac{t}{D}\right), \left(\frac{w}{D}\right), \left(\frac{S}{D}\right)\right\}. \quad (1)$$

Let $D_x$ be the diameter of the finned cylinder $x$ for which the value of $q$ is required and let $t_x$, $w_x$ and $S_x$ be the dimension of the fins and $V_x$ be the air velocity. Let $D_T$ be the diameter of the tested cylinders $T$ (4.66 inches). Define $J = D_x/D_T$.

[5] A. Fage, *Drag of Circular Cylinders and Spheres*, R. and M. No. 1370, British A.R.C., 1931.

Then by dividing all the dimensions of the finned cylinder $x$ by $J$ and multiplying the velocity by $J$

$$\left(D_T=\frac{D_x}{J},\ t_T=\frac{t_x}{J},\ w_T=\frac{w_x}{J},\ S_T=\frac{S_x}{J},\ V_T=JV_x\right)$$

a finned cylinder $T$ is regarded as set up in an air stream of velocity $V_T$ having the same value of the Reynolds number $\rho VD/\mu$ and of $\mu c_p/k_a$, $t/D$, $w/D$, $S/D$ as the finned cylinder $x$, and having a surface heat transfer coefficient $q_T$ which as seen from an inspection of Eq. (1) is related to the required surface heat transfer coefficient $q_x$ by the expression $q_x=(1/J)q_T$.

As it has been shown that $q_T$ is mainly a function of $V$ and $S$, it is only necessary to find $V_T$ and $S_T$ and to determine $q_T$ from Fig. 4.

A method for calculating $q$ for other altitudes will now be considered. The value of $q$ has been shown to vary with the 0.796 power of the velocity and to give this relationship Eq. (1) must take the form of

$$q=\frac{c_p}{D}(\rho VD)^{0.796}\mu^{0.204}\times f_1\left[\left(\frac{\mu c_p}{k_a}\right),\left(\frac{t}{D}\right),\left(\frac{w}{D}\right),\left(\frac{S}{D}\right)\right].$$

The quantities $\mu$, $c_p$ and $k_a$ depend on the temperature of the air, however, for the range of temperatures encountered in an ordinary altitude change $c_p$, $\mu c_p/k_a$ and $\mu^{0.204}$ are practically constant, causing a reduction in $q$ of only 3.5 percent for a variation of altitude from sea level to 25,000 feet.

Neglecting the effect of variation of $\mu$, $c_p$ and $k_a$ it is evident from the above equation that $q$ is a function of the mass flow $\rho V$, and that the value of $q$ at any altitude for a given finned cylinder is equal to the sea level $q$ for the velocity giving the same mass flow. When determining $q$ at other altitudes from the data presented it should be remembered that the density to which these data have been corrected is 0.0734 pound per cubic foot.

## Development of Heat Flow Equation

Referring to Fig. 6 the general equation for the flow of heat from a tapered fin, derived by equating the heat entering the element of volume by conduction radially and circumferentially to the heat carried away from the exposed surfaces of the volume by convection, is

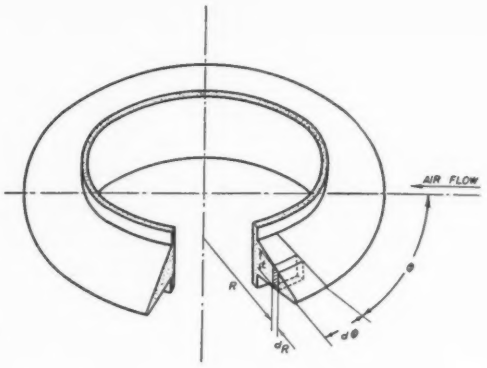


FIG. 6. Diagram of fin.

$$k\frac{\partial}{\partial R}\left(Rt\frac{\partial\theta'}{\partial R}\right)+k\frac{t}{R}\frac{\partial^2\theta'}{\partial\phi^2}=2q\frac{R\theta'}{\cos\alpha},\qquad(2)$$

in which

- $t$ is variable thickness of fin,
- $R$, radius to any point on fin,
- $\phi$, angular position of point from front of cylinder,
- $\theta'$, temperature at any point on surface of fin,
- $\alpha$, taper angle of fin,
- $k$, thermal conductivity of fin,
- $q$, surface heat transfer coefficient at any point.

In Eq. (2) the assumption is made that the temperature does not vary through the thickness of the fin. Harper and Brown have shown that the error introduced by this assumption is negligible for a thin rectangular fin.

The values of $q$, $t$ and $R$ in Eq. (2) vary from point to point on the fin and an exact solution of the equation would lead to an expression too cumbersome for practical use. Considerable simplification can be effected by replacing $R$, $t$ and $q$ by their average values. In general, the taper of the fins is so slight that $\cos\alpha$ can be taken as equal to 1. It will be shown later by a comparison of experimental values of heat dissipation with those calculated from the theoretical equation that the errors introduced by making these approximations are small.

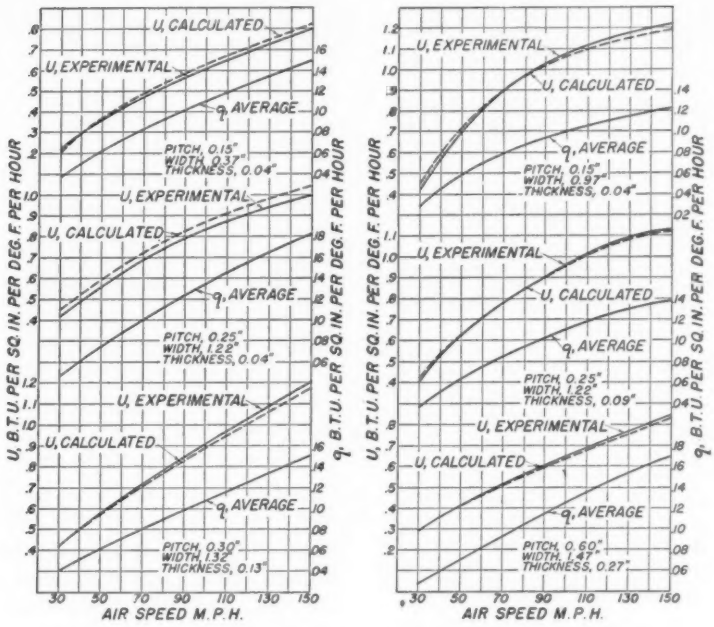


FIG. 7. Variation of average $q$ with air speed and comparison of calculated and experimental values of $U$ for six representative cylinders.

Introducing these simplifications in Eq. (2) and integrating with respect to $\phi$ from 0 to $\pi$ there results

$$ktR_a\frac{\partial^2}{\partial R^2}\left[\int_0^\pi \theta'\partial\phi\right]+\frac{kt}{R_a}\frac{\partial\theta'}{\partial\phi}\Bigg|_0^\pi = 2qR_a\int_0^\pi \theta' d\phi. \quad (3)$$

Since the temperature distribution around the fin is symmetrical with respect to the diameter parallel to the air stream, $\partial\theta'/\partial\phi=0$ at $\phi=\pi$ and $\phi=0$. Let $\theta$ be the average temperature of the fin at any radius then by definition

$$\theta=\frac{1}{\pi}\int_0^\pi \theta' d\phi$$

and Eq. (3) becomes

$$\partial^2\theta/\partial R^2=a^2\theta, \quad (4)$$

where $a^2=2q/kt$ and $t$ and $q$ henceforth designate the average fin thickness and average surface heat transfer coefficient, respectively.

Eq. (4) is similar to that for the straight rectangular fin and its solution is well known.

The heat dissipated from the fin tip can be accounted for as suggested by Harper and Brown by arbitrarily increasing the value of the width of the fin $w$ by one-half the tip thickness $t_t$. Define $w'=w+\frac{1}{2}t_t$. The solution of Eq. (4) is

$$\theta=\theta_b\cosh a(R-R_b-w')/\cosh aw', \quad (5)$$

subject to the conditions that $\theta=\theta_b$ when $R=R_b$ and $\partial\theta/\partial R=0$ when $R=R_b+w'$ where $\theta_b$ is the average root temperature and $R_b$ is the radius to the root.

The heat dissipated from the surface of a fin is in general

$$H_1=2\int_{R_b}^{R_b+w'}\int_0^\pi 2q\frac{\theta' R dR d\phi}{\cos\alpha}.$$

Introducing the same simplifications as made in the derivation of Eq. (4) and replacing $\theta$ by the expression given in Eq. (5) the following expression results:

$$H_1=[4\pi q(R_b+\tfrac{1}{2}w)/a]\theta_b\tanh aw'.$$

The amount of heat $H_2$ given off by that part of the cylinder wall exposed betwen two adjacent fins can be found approximately by assuming the wall surface heat transfer coefficient to be the same as that of the fins.

$$H_2 = 2\pi R_b S_b q \theta_b,$$

where $S_b$ is the length of cylinder wall exposed between two adjacent fins.

The heat dissipated per square inch of cylinder-wall area per degree of cylinder-wall temperature is therefore

$$U = \frac{H_1 + H_2}{2\pi R_b (S+t)\theta_b}$$

$$= \frac{q}{S+t}\left\{\frac{2}{a}\left(1+\frac{w}{2R_b}\right)\tanh aw' + S_b\right\}. \qquad (6)$$

It is now possible by means of Eq. (6) and the values of $q$ given in the preceding section to calculate the heat dissipated from finned cylinders. The experimental values of $U$ were compared with values calculated by means of this equation for various air speeds and for the various finned cylinders of which six representative cylinders are shown in Fig. 7. The agreement was found to be good for tapered fins as well as for rectangular fins.

## Optimum Fins

From Eq. (6) it is evident that there are a large number of fins of different dimensions which will dissipate the same quantity of heat from a cylinder for the same average cylinder temperature. These fins will differ in weight and it is desirable to derive a method for determining the lightest fin construction for a required heat transfer consistent with manufacturing practice.

For the purpose at hand, Eq. (6) can be simplified without introducing appreciable error by setting $S_b$ equal to $S$ and $w'$ equal to $w$. The value of $q$ can be replaced by a function of $S$

$$q = LS^n, \qquad (7)$$

where $n = 0.322$ and $L$ is a constant for a given velocity and density. (Cf. Fig. 4.) The volume of fin per unit of cylinder-wall area is given by

$$M = [wt/(S+t)](1+w/2R_b). \qquad (8)$$

$U$ in Eq. (6) may now be written as a function involving only $S$, $t$ and $M$ as variables.

$$U = \frac{LS^n}{S+t}\left\{\frac{1}{(2LS^n/kt)^{\frac{1}{2}}}\left[1+\left(1+\frac{2M(S+t)}{R_b t}\right)^{\frac{1}{2}}\right]\tanh R_b\left(\frac{2LS^n}{kt}\right)^{\frac{1}{2}}\left[\left(1+\frac{2M(S+t)}{R_b t}-1\right)^{\frac{1}{2}}\right]+S\right\}. \qquad (9)$$

Obtaining the partial derivatives of $M$ in Eq. (9) with respect to $S$ and $t$, respectively, and setting each equal to zero the following relations result:

$$\frac{S+(1+w/R_b)(S-n(S+t))}{S+(1+w/R_b)(S+n(S+t))}\tanh aw - aw\,\mathrm{sech}^2 aw$$

$$= as\left(\frac{1+w/R_b}{1+w/2R_b}\right)\left(\frac{t+n(S+t)}{S+(1+w/R_b)(S+n(S+t))}\right), \qquad (10)$$

$$\frac{S-(1+w/R_b)t}{S+(1+w/R_b)(2S+t)}\tanh aw - aw\,\mathrm{sech}^2 aw = as\left(\frac{1+w/R_b}{1+w/2R_b}\right)\frac{t}{S+(1+w/R_b)(2S+t)}. \qquad (11)$$

From a simultaneous solution of Eqs. (8), (9), (10) and (11) the values of $S$, $t$, $w$ and $M$ can be determined for the lightest fin construction which will dissipate a required amount of heat $U$. These calculations lead to fins which are much too thin and too closely spaced to be considered practical.

The problem is then to determine the dimensions of the fins of minimum weight to dissipate a required amount of heat subject to the addi-

tional conditions that the fin thickness and space be not less than the values set as manufacturing limits. For a specified fin thickness $t$ and a given heat dissipation $U$, the required values of $S$, $w$ and $M$ can be obtained from a solution of Eqs. (10), (9) and (8). These quantities were calculated for a range of values of $U$ and specified fin thickness, $t$, and are shown plotted in Fig. 8. The criterion of the weight economy $(U/M)$ was also plotted in the figure. If $S$ is specified instead of $t$ then for a given value of $U$ the values of $t$, $w$ and $M$ can be obtained from a solution of Eqs. (11), (9) and (8). These quantities were calculated for a range of values of $U$ and specified space $S$ and are also shown plotted in Fig. 8. The values of $q$ used were obtained from Fig. 4 for a velocity of 76 miles per hour.

In practice limits will be set for both the minimum allowable fin spacing and thickness. For these specifications a result can be obtained from each chart in Fig. 8 for a required value of $U$. Not more than one of these results will give dimensions sufficiently large to completely satisfy the specifications and be a solution of the problem.

In cases when neither chart gives a solution and only in such cases, the fins of minimum weight can be found by substituting the values of $U$ and of the specified minimum thickness and spacing in Eq. (6) and solving for $w$.

An examination of Fig. 8 shows that the lower the specified minimum thickness and spacing the lighter are the fins which can be used to dissipate a given amount of heat. The curves also indicate that for a specified fin spacing the heat output can be increased by increasing the thickness and width, and that this gain is made at a sacrifice of weight economy, while for a specified thickness the heat output can be increased by decreasing the spacing and slightly increasing the width. For the latter case there is little loss in weight economy. Similar charts have been plotted for other air speeds, cylinder diameters, and metals, and indicate the same trends.

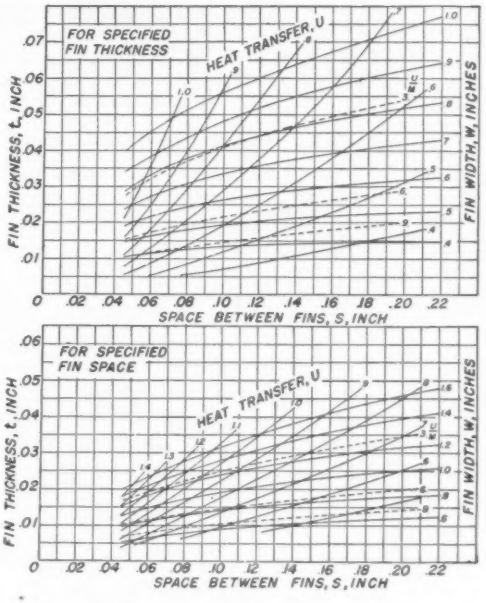
FOR SPECIFIED FIN THICKNESS
HEAT TRANSFER, U
FIN THICKNESS, t, INCH
FIN WIDTH, W, INCHES
SPACE BETWEEN FINS, S, INCH
FOR SPECIFIED FIN SPACE
HEAT TRANSFER, U
FIN THICKNESS, t, INCH
FIN WIDTH, W, INCHES
SPACE BETWEEN FINS, S, INCH

FIG. 8. Optimum fin dimensions for the condition in which the fin thickness is the specified governing dimension and for the condition in which the fin space is the governing dimension. ($V=76$ m.p.h., $D=4.66$ in., $k=2.17$ B.t.u. per deg. F per in. per hr.)

The results of recently completed tests, now being prepared for publication, show that the equations presented here can also be applied to shrouded cylinders and to blower-cooled cylinders when the values of $q$ for these cases are available.

# Recent Aspects of Stressed Skin Construction

EARLE E. BLOUNT, *Wright Field, Dayton, Ohio*

(Received July 1, 1934)

THE subject of stressed-skin construction is too vast to be covered in its entirety in a paper of this sort. The author hopes, however, to present some ideas and information on several phases of the problem which will prove of real value to the designer and which may suggest specific topics for further research. The subtopics to be considered are: The proportioning of flat sheet with stiffener reinforcement, criteria for stiffener design, corrugated sheet design, the important objectives to be sought for in stressed-skin construction, a hybrid type of wing construction, comparison of stainless steel and dural, and lastly the effects of size and compactness of construction.

Of course the primary object of stressed-skin construction is to utilize the covering or skin of an aircraft body, which must exist to fulfill the shape of the body, for carrying stresses which would otherwise require additional structural material. It is generally agreed that there are no difficulties involved in carrying tension in the skin, the only thing to keep in mind being the need for continuity of material at the joints or splices. Where the skin is moderately thick, shear is as easy to carry as tension, and in very thin-skinned structures, shear may be readily and efficiently carried by a diagonal tension field, as it is in the web of a Wagner beam. The only difference between the plate and tension field is that in the unsupported plate the compressive component of stress at 45° to the shear is carried in the plate itself, whereas in the tension field the skin is too thin to carry any compression and must be divided into rectangles with stiff members along the edges of each panel to take the compression.

In our enthusiasm for a new type of construction I am afraid we have let the suggestiveness of our terminology carry us too far. The inherent efficiency implied by the phrase "stressed skin" has led to an attempt to carry every kind of stress in the skin, including compression, for which it is distinctly unsuited. However, it may be made to help greatly in carrying compressive load, with careful design. Extensive studies have been made of ways of reinforcing metal skin to enable it to carry higher compressive stresses. The idea is to carry the load in the skin by devoting a suitable percentage of the total material to skin-supporting stiffeners. This approach gives satisfactory results for small structures subjected to heavy loads, where the ratio of skin thickness to other dimensions may be comparatively great, but it fails to reveal the best possibilities for larger and relatively lighter structures. In the latter case it is better to design the stiffeners to carry the compressive load and use the skin to so reinforce and support them that they will withstand much higher stresses than otherwise. The following is a concrete example: Assume a 100,000-pound compressive load to be supported by a strip of dural 100 inches wide. The column length (determined by the desired rib spacing) is 19 inches, but could be varied somewhat from that in either direction if necessary. Design may be begun by dividing the 100 inches into 20 five-inch strips by stiffeners. Five inches is not far from the optimum spacing in this case. First, two-thirds of the metal will be put into the sheet and one-third into stiffeners, and then the distribution will be reversed. Assume 0.040-inch thickness. The maximum load a 0.040-inch strip can carry is 1700 pounds regardless of width.[1] The twenty strips can then carry 34,000 pounds at most. Area of the sheet is four square inches; therefore, two square inches will be put into the nineteen stiffeners. The outer edges of the 100-inch panel are assumed to be restrained by other means. Area of each stiffener equals 0.105 square inches, which just fits a hat-shaped section approximately 1 inch by $\frac{3}{4}$ inch with $\frac{3}{8}$-inch flanges turned out at the foot and 0.030 inch thick, as shown in Fig. 1. $\rho$ is approximately 0.38 inch and $L/\rho = 50$. This stiffener will carry a compressive stress of about 25,000 pounds per square inch.[2] The total allowable load on the

[1] See N. A. C. A. Report No. 356.

[2] Compare with top curve, page 157, Niles and Newell, or page 7, A. C. I. C. No. 598.

stiffeners is therefore 50,000 pounds, and the allowable load for the combination is 84,000 pounds, which is not enough.

For the alternative design a skin thickness of 0.020 inch will be assumed and a total stiffener area of four square inches. Each strip of sheet may carry 430 pounds, making 8600 pounds in the sheet. The stiffeners will have an area of 0.21 square inch each, which fits a hat-shaped section $\frac{3}{4}$ inch by $1\frac{1}{2}$ inch with $\frac{3}{8}$-inch flanges and 0.045 inch thick. A groove should be made down the middle of each side to prevent local buckling. $\rho$ is about 0.56 inch and $L/\rho$ about 34. These stiffeners will carry at least 30,000 pounds per square inch and probably much higher. Total allowable load in stiffeners equals 120,000 pounds and total for the combination is 128,600 pounds, or 53 percent more than the first case.

The allowable loads used for the 5-inch strips are a little high, because a 5-inch strip will carry only about 90 percent of the maximum load for unlimited width strips, but this only makes the comparison stronger. Another method of computing the strength of the panel would be to assume that the sheet behind each stiffener carries the same stress as the stiffener and to estimate the average stress in the strips between stiffeners, but the results would be the same, showing a distinct advantage for the thin sheet and heavy stiffeners. Other metals show the same trend. Tests on a great many stainless steel specimens of every conceivable combination of sheet thickness and stiffener thickness, width, depth and spacing, made recently at the Material Division, indicate that if a strip of sheet slightly wider than the stiffener is considered to carry the same stress as the stiffener, then the rest of the sheet carries nothing. The average stress in the sheet usually fell between 15,000 pounds per square inch and 50,000 pounds per square inch for reasonable skin thicknesses and stiffener spacings, whereas it is possible to develop in this metal (in corrugated sheet of $R/t=33$ and $L/\rho=23$) as high as 196,000 pounds per square inch compressive stress. Stiffeners developed from 105,000 pounds per square inch to 135,000 pounds per square inch and might, with careful design, be made to go higher. The inefficiency of using heavy sheet can be further illustrated by two alternative designs in stainless steel. Let

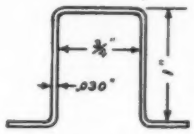


FIG. 1.

FIG. 2.

the first consist of 0.030 inch sheet with 60 percent of the metal in the sheet. With stiffener spacing of about 6 inches, the sheet will probably average about 30,000 pounds per square inch and by keeping $L/\rho$ down the stiffeners can be made to develop 120,000 pounds per square inch. Average stress for the combination is $0.6\times30{,}000+0.4\times120{,}000=66{,}000$ pounds per square inch. In the second design, the sheet thickness will be cut to 0.010 inch, throwing 80 percent of the material into stiffeners. The 0.010 inch sheet will probably carry an average stress of 17,000 pounds per square inch, making the average for the combination $0.2\times17{,}000+0.8\times120{,}000=99{,}400$ pounds per square inch. In this comparison the same allowable stress for stiffeners was used in both cases, although the stiffeners containing more metal will undoubtedly carry higher stresses. The point illustrated is, why put most of the metal into the sheet when, as stiffener material, it will carry much higher stresses? As a general principle of design, the following might be suggested: Make the skin as thin as is practical and put enough material into stiffeners to carry the compressive load. The only exceptions to that are cases where the skin has a very small radius of curvature, or where the structure is small and subjected to heavy loads requiring so much material that the stiffeners can be spaced almost touching each other.

The conclusion to be drawn from the foregoing is that the design of stiffeners to carry compressive load is more worthy of careful study than the reinforcement of thin sheet so that it can carry compressive load. More attention might well be directed toward this phase of the subject. All of the stiffeners in the recent tests at the Material Division were of the general shape shown in Fig. 2. When the depth was greater than one inch there were grooves in the side plates every half inch. This section is easy

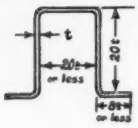


FIG. 3.

FIG. 4.

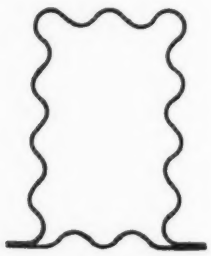

FIG. 5.

and cheap to build when the components are spot-welded together, but it has the weakness of possessing a number of outstanding free edges. Failure was frequently started by waviness developing in the free edges. Another weakness is that the grooves are not deep enough to completely stabilize the side walls. In specimens where the skin was very thin, the free edges next to the skin were first to fail, having insufficient support in the combined thickness of skin and stiffener. Paradoxically the specimens with very thick skin and thin stiffeners failed in the same place, apparently because the forces in the skin, when it formed its normal wrinkle pattern, were so great that they were able to distort the stiffener and cause it to buckle along with the skin;—another argument against thick stress-carrying skin and light stiffeners. In designing to the minimum practical skin it may be advisable to put a strip of the same thickness as the stiffener directly behind the stiffener, as shown in Fig. 5, to increase $\rho$ and help stabilize the free edges next to the skin, thus making a closed section of the stiffener. This strip will have the same grooves or corrugations as the stiffener itself.

Figs. 3 and 4 show simple stiffeners suitable for small structures with moderate to heavy loads. In very large structures where it is impractical and inefficient to place the ribs or bulkheads close together these sections will have a prohibitively high $L/\rho$. To increase $\rho$ by simply making them thinner, wider, and deeper will not do because the increased flat sides would buckle locally. Fig. 5 shows a section which will carry high compressive stresses, but which complicates joint design considerably and is difficult to make in a stiff metal of indefinite yield point like stainless steel. The use of hexagonal or square corrugations instead of the circular arc corrugations would remove this last objection, but would also lower the allowable stress somewhat. It is questionable whether as high stresses can ever be developed in a section containing flat sides as can be in one of continuous curvature. In extremely large structures it may be feasible to build up a stiffener with flat sides reinforced by smaller stiffeners. Such practical considerations as cost of frabrication are of utmost importance in stiffener design.

While mentioning the design of stiffeners, it may be well to bring up some discoveries made recently regarding optimum pitch-depth ratios in corrugated sheet design. If corrugated sheet is used beneath thin flat skin in an aircraft surface, it acts both as stiffener and, in certain respects, as skin. The prime consideration in using corrugated sheet as a structural member or as part of a structural member is, of course, to obtain the greatest strength with the minimum possible weight. All comparisons will, therefore, be made on the basis of sections of equal weight, or, what is the same thing, of equal cross-section area. Consideration will be limited to corrugations made up of equal circular arcs, for reasons given later. If a strip of flat sheet of fixed width $W$ is compared with a strip of corrugated sheet of the same width $W$ as shown in Fig. 6, it will readily be seen that the corrugated sheet for any given thickness $t$ will have a greater cross-section area and greater weight than the flat sheet. The increase in weight, or ratio of weight to that of flat sheet of equal width and thickness, can be obtained from a chart in the Army handbook (Fig. 140 on page 273). In order to keep the weight of the sections constant, the corrugated sheet must be made thinner than the flat, and the deeper the corrugations, for any given pitch, the thinner must be the sheet. Thus we can plot thickness against pitch-depth ratio, for sections of constant weight, as was done in

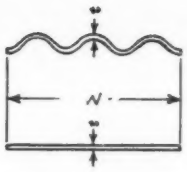


FIG. 6.

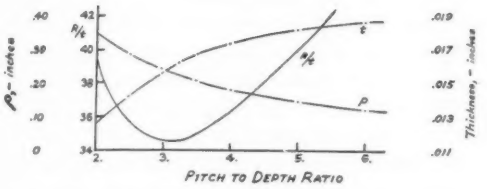


FIG. 7. Properties of constant weight corrugated sheet. $R$=radius of curvature, $\rho$=radius of gyration, $t$=thickness. Plotted for pitch=2 inch and equal weight flat sheet thickness=0.020 inch. For other pitches, multiply $R/t$ and $\rho$ by the ratio of pitches. For other thicknesses, multiply $R/t$ by the inverse ratio of thicknesses and multiply $t$ by the direct ratio of thicknesses.

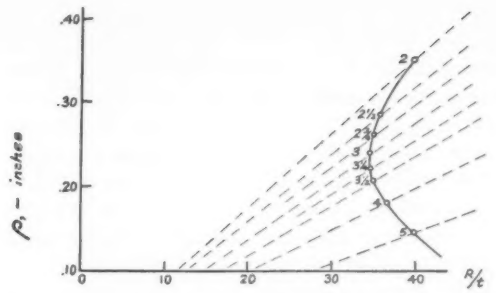


FIG. 8. Variation of $\rho$ with $R/t$ for constant weight sheet. Values of $P/D$ are spotted along the curve. Plotted for pitch=2 inch and equal weight flat sheet thickness =0.020 inch. For other pitches, multiply both $R/t$ and $\rho$ by the ratio of pitches. For other thicknesses, multiply $R/t$ by the inverse ratio of thicknesses.

Fig. 7. It should be noted that the thickness for constant weight depends only on pitch-depth ratio and not in any way upon the absolute magnitudes of the pitch and depth.

It is universally known that the strength of corrugated sheet metal in compression depends greatly on the ratio of radius of curvature $R$ to thickness $t$ especially in the short column range. It is important to keep $R/t$ as low as possible. Now if the depth of the corrugations is increased, keeping the pitch constant, we will get smaller and smaller values for $R$. But at the same time the thickness for constant weight is decreasing, and in the lower values of $P/D$ it decreases faster than $R$ so that the curve of $R/t$ turns up again, as shown in Fig. 7. This means that where buckling strength alone is concerned, there is an optimum pitch-depth ratio ($3\frac{1}{8}$) at which the metal is most efficiently used to give the lowest $R/t$ possible. Once the $P/D$ ratio is fixed, $R/t$ varies directly as $P$ and inversely as $t$.

It is not practical, however, to decrease $R/t$ indefinitely by decreasing $P$, for the radius of gyration $\rho$ also varies directly with $P$, and is fully as important in influencing compressive strength as $R/t$. For maximum column strength it is desirable to have $\rho$ and therefore $P$ as large as possible; for maximum buckling strength it is desirable to have $R/t$ and therefore $P$ as small as possible, and practical considerations may influence our choice of a compromise. But in selecting pitch-depth ratio, there is no conflict for the ratio down as low as $3\frac{1}{8}$. As will be seen from Fig. 7, in decreasing $P/D$ to $3\frac{1}{8}$, $\rho$ increases and $R/t$ decreases, so that there is never any reason for using $P/D$ greater than $3\frac{1}{8}$ unless the sheet is being used as a non-structural covering where $t$ is a practical minimum, and in that case a slightly thicker or reinforced flat sheet would probably be more suitable.

If $\rho$ is plotted against $R/t$ for constant weight sections, as in Fig. 8, we find minimum $R/t$ represented by the vertical portion of the curve, where $\rho$ changes rapidly with very little change of $R/t$. The dotted lines through the origin represent the variation of the values of $\rho$ and $R/t$ that would be caused by varying pitch. Thus for each pitch-depth ratio, $\rho$ and $R/t$ bear a constant ratio to each other and both can be increased or decreased along the dotted line by increasing or decreasing $P$. If it is desired to increase $\rho$ to obtain greater column strength this may be accomplished either by increasing $P$ and going up the dotted line or by decreasing $P/D$ and going up the curve. Obviously the latter gives more $\rho$ with less sacrifice of buckling strength. The best $P/D$, from the standpoint of obtaining $\rho$ with the least cost in $R/t$, would be the $P/D$ corresponding to the point of tangency where a dotted line from the origin is tangent to the upper surface of the curve. From this point

on, $\rho$ could be obtained with less cost in $R/t$ by going up the dotted line of increasing pitch instead of the curve of decreasing $P/D$. However, this point of tangency lies just beyond $P/D=2$, which is the lower limit in manufacturing circular arc corrugations by practical methods. Therefore, a pitch-depth ratio of 2 should always be used when column strength is of prime importance, and the pitch should be increased or decreased until the column strength and buckling strength of the specimen are just equal.

If the thickness $t$ were doubled, the curve in Fig. 8 would shift to the left until it was only half as far from the vertical axis through the origin, but at the same time all horizontal distances between points on the curve would be cut in half, so that the ratio of slope of curve to slope of dotted line would remain the same and the point of tangency would still be just beyond $P/D=2$.

Although the theoretically best $P/D$ when there is absolutely no column action whatsoever involved is $3\frac{1}{8}$, this circumstance probably never occurs in practice. No matter how short the specimen, there is some small column effect existing. Since a pitch-depth ratio of 2 will give the desired $\rho$ with the least sacrifice in $R/t$ or will give the desired $R/t$ with the least sacrifice in $\rho$, this ratio is recommended whenever corrugated sheet is used as a structural member. Circular arc corrugations are considered best for compression because they have a constant radius of curvature. Other shapes with varying curvature would (since a structural member is no stronger than its weakest portion) be only as strong as the portion with greatest radius of curvature. For members subjected primarily to bending, so that the stress at the crests of the corrugations is considerably higher than elsewhere, another curve having smaller curvature at the crests, such as the parabola, for example, might be more suitable.

So far consideration has been limited to the nominal object of stressed-skin construction, to make the skin a part of the primary structure, and make it carry load. There are two other objects of stressed-skin construction which, under special circumstances, may be considered more important than this one: first, to make the skin, either stressed or unstressed itself, so support and strengthen members of the primary structure as to enable them to carry much higher loads than they otherwise could, and second, to redistribute loads by action of the skin so that the primary structure can function more efficiently. One case of this first special object was seen in the design of stiffeners, where the stiffener was made somewhat deeper than it is wide because the skin prevents it from bowing sideways. In Wagner beams where the vertical stiffeners are attached to the web, they will be found to carry much more compression than the column formulae indicate, because the tension field web restrains them from bowing not only in the plane of the web but perpendicular to it as well. The same principle applies when the airplane skin acts as a tension field.

The second special object of stressed-skin construction applies particularly to airplane wings. In the conventional two-spar construction the air load is divided between spars in inverse proportion to their distances from the center of pressure. If the C.P. were always midway between spars, the air load would divide equally between them and they could be very efficiently designed, but unfortunately the C.P. shifts from close to one spar in some conditions of flight to close to the other in other conditions, necessitating the design of each spar for a high percentage of the total load in some critical condition. The use of the "Box Spar" or stressed-skin type of construction eliminates this necessity. Somewhere in the wing, normally between the front and rear spar locations, is an elastic axis such that, if all the air load were applied along this axis, the wing would deflect without twisting. If, instead of dividing the air load between the spars, we conceive of it as a force acting through this elastic axis plus a torsional moment about this axis, we have a clearer approach to the problem. This conception is just as applicable to the conventional two-spar construction, where the torsional moment is represented by a vertical couple which increases the load on one spar and decreases it on the other. In the stressed-skin wing this torque is not taken entirely by the spars or webs; approximately half of it is carried by the upper and lower skin. This means that the shear in the critical web will be half-way between what it would be if the air load were divided

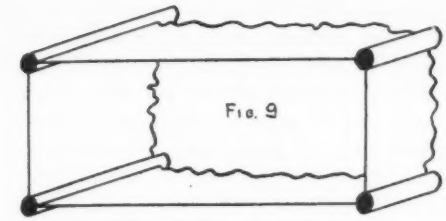

FIG. 9

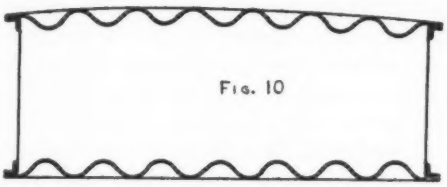

FIG. 10

equally between webs and what it would be under the conventional two-spar division of load. But it is not this reduction of shear that is the greatest advantage effected by the stressed-skin construction. It is the fact that the shear in the web and the shear in the skin have opposing effects on the flange material. In a symmetrical rectangular box, such as is shown in Fig. 9, where the web and skin are of equal thickness, these opposing influences exactly balance and the stress in the corners, due to an applied torque, is zero. This means that the compression and tension flange material can be distributed as it would be if the air load were always divided equally between webs. In the conventional box beam, such as the one shown in Fig. 10, the flange material is spread over the upper and lower surfaces between webs, thus reducing the shearing stresses in the upper and lower surfaces to very low magnitudes. However, it is not at all necessary to spread it out in this manner, and in large size structures, efficiency is lost by doing so. The most important gain from the box-type construction, and the one that should be retained at all costs is the getting of all the flange material to work against all the beam load in every condition. The reduction of shearing stresses due to torque is relatively unimportant. With the flange material concentrated at the corners, the main objective is still accomplished, for the torque, caused by the air load not being centered on the elastic axis, is carried by shear in the webs and skin, and the stress in the flange material induced by this extra shear in the webs is exactly neutralized by the stress induced by the shear in the skin. If the webs and skin are not of equal thickness or are of different materials, this does not hold precisely, but the qualitative effect is there. In large wings, especially those of modern airfoil section with relatively stable center of pressure, the minimum skin thickness which it is practical to use has more than enough cross-sectional area to carry all the shear due to torque, particularly if the skin is reinforced so that it can resist this shear as a diagonal tension field. If the skin is further thickened by adding flange material to it, an unnecessary reduction in shear stress is accomplished and the only advantage obtained is a slight increase in torsional rigidity of an already highly rigid wing. But the disadvantages resulting from this inefficient use of flange material are serious. If corrugated sheet is used as flange material, in order to carry high compressive stress, $L/\rho$ must be small, and, since the cost in rib weight of breaking up corrugations into very short columns by close rib spacing is prohibitive in a thick wing, this means deep corrugations which have a high $\rho$. But in a large wing with a limited amount of flange material desired and a great width between webs to spread it over, the corrugated sheet will be so thin that deep corrugations mean high $R/t$ and low buckling stresses. If flat sheet with stiffeners is used as flange material, the disadvantages are reduced, but are still serious. With stiffeners spaced far apart it is not so hard to concentrate enough material in each stiffener so that with good detail design the danger of local buckling is eliminated, but to obtain low enough $L/\rho$ the stiffeners must be so deep as to interfere seriously with the necessary chord-wise members. Also, large stiffeners designed against local buckling are hard to attach to other members.

If all the flange material is concentrated at the webs, it still acts unitedly to resist the total bending moment on the wing, and the main purpose of the box construction is achieved. One of the arguments sometimes heard against such design is that it necessitates extra material as secondary structure to support the skin between spars and maintain the contour of the wing, but this is not necessarily true. A good deal of chordwise material is needed to carry

loads from the nose ribs and overhang behind the rear spar, and this can be used to shape the skin just as effectively as the flange material. When a very thin skin is used and torque shear and drag shear are carried in a diagonal tension field, this tension tends to pull the spars together and a considerable amount of additional chordwise material is needed to carry the compression. When the skin between webs is free from spanwise material, except for small discontinuous secondary stiffeners, these chordwise compression members can be simple, efficient, and cheap to make. This construction, which might be called "two-spar stressed skin" to distinguish it from the pure box type, permits the wing surface between spars to be made up of large detachable rectangular panels, if desired. The spars would be connected at intervals by complete ribs containing diagonal bracing to prevent twisting of one spar with respect to the other. Between these ribs, the rectangular panels of skin would have deep chordwise stiffeners, but no members running from upper to lower surface. In a very deep wing, say 5 or 6 feet, the economy of omitting members connecting upper and lower surfaces is considerable.

Attempts have been made to cut down the amount of material necessary in chordwise members by using a multi-web box construction. While this may be quite practical in a small wing, it is not satisfactory in the very large sizes. The inner webs are inefficient so far as helping to carry the torque is concerned, and unless we are willing to abandon the main purpose of the box construction, that is, the equalization of stress due to bending, throughout the flange material, we must put in nearly as much chordwise material as would be required in a two-web wing. The saving in chordwise material will be offset by the additional weight of the extra webs, particularly in thick wings where the design web thickness for a two-web construction is apt to be close to the minimum practical thickness.

The choice between stainless steel and dural is difficult to make. In general, compact construction and heavy loading tend to throw the balance in favor of steel, while large size, spread-out construction, and light loads tend to favor dural. Heavy loading can be caused by high wing loading, high load factor, or both, or by structural constriction, an example of which would be thinness of a wing subjected to bending. Each case must be examined individually and the project must be carried almost to the point of detail design before a decision of any value can be made. In tension, the balance seems to be slightly in favor of steel with tensile strengths of from 180,000 to 200,000 pounds per square inch, although these stresses can seldom be obtained from strips over 0.060 of an inch thick. In compression, the greater bulk of dural tends to give it some advantage. The use of dural means three times as much volume with the same weight and strength, and in large structures this makes it easier to obtain a suitable $L/\rho$ without danger of local buckling. However, this advantage is largely neutralized by the low modulus of elasticity of dural. Assuming the ultimate tensile strength of stainless steel to be three times that of dural, a steel column of $L/\rho = 100$ will carry the same percent of ultimate stress as a dural column of $L/\rho = 76$; a steel column of $L/\rho = 70$ will carry the same as a dural of $L/\rho = 45$; and steel $L/\rho = 50$ is equivalent to dural $L/\rho = 27$. In cases where member sizes are determined by the practical minimum rather than by design loads, dural is always better. Design by practical minimums is by no means limited to small airplanes, but occurs frequently in very large structures. Sometimes the practical minimum increases with the size of the structure, as, for example, in the case of bulkheads in a cylindrical structure, or very lowly stressed verticals in a wing rib.

In comparing weights, the fact must not be overlooked that dural requires considerable protective coating to prevent corrosion. On wings this may amount to 6 or 8 percent of the total wing weight. If stainless steel is used it will probably be spot-welded, whereas in dural the normal construction at present is riveting. A considerable saving in weight is made by the elimination of rivet heads and many of the gusset plates, and in tension members much structural efficiency is gained by eliminating rivet holes. A considerable aerodynamic advantage, the reduction of drag, is gained by the elimination of rivet heads. Dural may also be spot-welded, but the cost is greater than in stainless steel, due to the heavier current re-

quired. One of the present disadvantages of stainless steel is that very thin sheet cannot be obtained in strips over 6 or 8 inches wide without sacrificing uniformity of thickness, due to deformation of the rolls. The tensile strength and modulus of elasticity are somewhat greater across the grain, but with such narrow strips it is impractical to form cross grained structural members. There is no reason why dural and steel should not be used together in a structure, each where it is most suitable. For example, a wing might be made with stainless steel spars, dural nose, dural cover panels between spars, and fabric covered dural rib overhang back of the rear spar. In a large wing the cover panels would be reinforced by deep dural chordwise stiffeners or semi-ribs, but the upper and lower panels would not be connected except at the ends where there would be a full rib. The danger of electrolytic action between steel and dural is easily eliminated by a protective coating of bitumastic paint or impregnated fabric where they come in contact, and the difference in coefficient of thermal expansion is not serious. If a member composed of steel and dural, intimately connected, is subjected to a temperature change of 100°F, say from +60°F to −40°F, and infinite rigidity is assumed in the steel so that it shrinks its normal amount uninfluenced by the dural, then there will be an induced tension of 7000 pounds per square inch in the dural. Actually, the steel would compress somewhat, depending on the relative amounts of steel and dural, and the induced stresses would be lower.

Most of the remarks regarding the inefficiencies involved in spreading out flange material too thin apply particularly to stainless steel. The disadvantages are not so great with dural. However, with either metal there is much to be gained by keeping the structure as compact as possible. In a wing of the single box spar type this may consist chiefly of bringing the rear web forward far ahead of the conventional rear spar position. For a fairly stable airfoil 40 percent or 45 percent of the chord should not be too far forward. This may bring the elastic axis very close to the average C.P. and thus reduce the applied torque as well as promote structural efficiency. Single box spars with a width-depth ratio in the neighborhood of $1\frac{1}{2}$ to 1 should be very common in future design. Reduction of the cross-sectional area included by the box should cause an increase in shear stress due to torque, according to the familiar formula $S=Q/2At$, but the simultaneous thickening of the upper and lower skin to maintain a constant amount of flange material will neutralize this effect. If the "two-spar stressed skin" type construction or skin and stiffener construction is used, and the skin is kept at the practical minimum, there will be no neutralizing effect, but since in this case the skin is too thin to carry any compression and will be used only as a tension field, then it will be economy to stress it up closer to its ultimate than the conventional wide box would stress it, anyway.

If the arbitrary decision is made to use fabric covering aft of the rear web, much weight is saved by using the narrowest possible box, the difference between fabric and minimum metal covering being roughly $\frac{1}{4}$ of a pound per square foot per surface. Metal skin on the rear half of the wing adds very little either to bending or torsional strength or stiffness.

As a further example of the advantage of compact construction, a few computations from the design of a certain very large fuselage will be considered. Assume the fuselage is cylindrical and that the bending moment from tail loads at the section under consideration is 2,000,000 inch-pounds. Torsion in this case is not critical. The possibilities of pure monocoque construction will be investigated first. Trying a dural section of 80-inch diameter and 0.080-inch wall thickness, we find: $R/t=500$. Allowable fiber stress in bending (from N. A. C. A. Technical Note 479) is $0.000476\times10{,}500{,}000=5000$ pounds per square inch. $I/y=\pi r^2t=402$. Allowable bending moment $=402\times5000=2{,}010{,}000$ inch-pounds. Now if the diameter is reduced and at the same time the wall thickness is increased to keep the weight constant, the comparison given in Table I between large and small sections of the same weight can be made.

By cutting the diameter in half, $2\frac{1}{2}$ times as much allowable bending moment is obtained for the same weight. This is just opposite to the principles governing the design of small tubes, where the allowable bending moment can be

TABLE I. 1, diameter and wall (in.); 2, $R/t$; 3, allowable stress×lb./sq. in.; 4, $I/y$; 5, allowable moment×in.-lb.

| 1 | 2 | 3 | 4 | 5 |
|---|---|---|---|---|
| 80×.080 | 500 | 5,000 | 402 | 2,010,000 |
| 64×.100 | 320 | 8,930 | 322 | 2,875,000 |
| 40×.160 | 125 | 25,500 | 201 | 5,120,000 |

increased by increasing diameter and reducing thickness. It shows what a difference size can make in the principles governing design. For tubes in pure bending, the optimum $R/t$ is in the neighborhood of 60. In compression, of course, it pays to go below this if possible.

If instead of maintaining constant weight we design for the required bending moment, it is found that a 40 inch×0.105 inch cylinder will carry 2,047,000 inch-pounds bending moment and has only 65 percent the weight of the 80 inch×0.080 inch cylinder. Of course the torsional rigidity is less, but will probably be more than ample even in the smaller cylinder. An increase in effective shearing modulus of elasticity, due to thicker walls, partially compensates for decrease in size and keeps the loss of torsional rigidity from being great.

Let us next examine a construction consisting of longerons, bulkheads, and the minimum practical skin. A few secondary stiffeners may be necessary, but will not affect the comparison. Assume a depth between the longerons of 80 percent the cylinder diameter, an allowable longeron stress of 35,000 pounds per square inch, and that it seems inadvisable to use less than 0.020-inch skin thickness. For the 80-inch cylinder, longeron load = 2,000,000/64 = 31,300 pounds, and longeron cross-section area 2 ×31,300/35,000 = 1.79 square inches. Skin area is $80\pi(0.020) = 5.02$ square inches and total area = 6.81 square inch. Weight per inch length = 0.654 pound per inch. Comparing this with two smaller cylinders we have:

TABLE II.

| Diameter (in.) | Longeron Load (lb.) | Longeron Area (sq.in.) | Skin Area (sq.in.) | Total Area (sq.in.) | Weight (lb./in.) |
|---|---|---|---|---|---|
| 80 | 31,300 | 1.79 | 5.02 | 6.81 | 0.654 |
| 64 | 39,100 | 2.23 | 4.02 | 6.25 | 0.600 |
| 40 | 62,500 | 3.57 | 2.51 | 6.08 | 0.584 |

Bulkhead weight is also reduced by using smaller diameter.

The lesson for intermediate types of construction, generally classed as semi-monocoque, is the same. Whether corrugated sheet or flat skin with stiffeners is used, overall size should be kept fairly low. The actual case which suggested these comparisons is of an elliptical fuselage, but the results are the same and circular cylinders are used here to simplify calculations. The weights of the 80-inch and 40-inch monocoque fuselage were, respectively, 1.93 pounds per inch length and 1.265 pounds per inch, suggesting again the inferiority of monocoque construction in large sizes.

# The New Whirling Arm

TH. TROLLER, *The Daniel Guggenheim Airship Institute*

(Submitted August 1, 1934)

## Introduction to Th. Troller's Paper on Experimental Research at the Daniel Guggenheim Airship Institute

TH. VON KÁRMÁN

In addition to grants awarded to several American educational institutions engaged in aeronautical research, the Daniel Guggenheim Fund for the Promotion of Aeronautics decided in 1929 to erect a special research institute for the investigation of problems associated with the design and operation of lighter than air craft. It was decided that the institition should be allied with the University of Akron, and the city of Akron made a material contribution to the project, especially in regard to the expenses of erecting a new building. Harry F. Guggenheim, George F. Zook, President of the University of Akron, Jerome Hunsaker, and R. A. Millikan were instrumental in giving a definite shape to the new organization. In the fall of 1930 the present writer was appointed Director of Research of the Institute and Th. Troller, Assistant Director, residing in Akron.

The research program of the Institute is comprised of aerodynamics, instruments, metallurgy and meteorology. In the following paragraphs, ideas underlying the choice of the problems directly attacked or to be attacked, are briefly indicated.

(a) *Aerodynamics.* It was felt that our knowledge of air forces in the case of airfoils is more complete and theoretically better founded than in the case of airships. Hence a series of investigations was started with the purpose of studying the aerodynamical mechanism of dynamic lift and stability. The problem of the drag of airships was recognized as being of great importance; however, the size of the wind tunnel was restricted by the funds available, and it is known that the extrapolation of wind tunnel data on drag of airships is even difficult in the case of the largest existing wind tunnels and of those operating with compressed air. Consequently, it was decided to study the drag problem from the standpoint of the boundary layer theory and to restrict the experimental research to boundary layer investigations, to experiments on the drag of protruding parts, ventilation openings, etc. The problems of air forces acting on a stationary ship in a natural wind was chosen as one of the research problems in view of its importance for ground handling of airships. Theoretical investigations carried out by research fellows of the Institute had the object of calculating the magnitude of air forces to be expected in flight through gusty air, especially through a vortex field.

(b) *Instruments.* Study and eventual improvement of instruments used in the operation of airships is considered as one of the important tasks of a special Lighter than Air Institute. As an example, the development of exact and simple methods for measurement of the density of lifting gases may be mentioned.

(c) *Metallurgy.* Concerning structural problems, it was felt that the limited space available as well as the financial means of the Institute would not allow extended research work on actual structures or structural elements. It is known that such work has been done and is being continued at present with success, in research laboratories of airship manufacturers. Hence, it was decided to concentrate the efforts, as far as the structural field is concerned, on metallurgical problems. In view of its importance in the future, the problem of spot-welding was chosen as a paramount question.

(d) *Meteorology.* The importance of meteorological research for aircraft operation is recognized by all concerned; especially the meteorological characteristics of the lower sheets of the atmosphere. The characteristics of the boundary layer next the ground are perhaps of greater importance for the operation of airships than for that of airplanes.

Below is presented a part of a progress report on research work at the Daniel Guggenheim Airship Institute, written by Dr. Troller. In a few months reports concerning some of the problems mentioned above will be published.

---

ONE of the outstanding problems in the design of airships is the determination of the distribution of air forces acting on the ship under the different conditions to which it is subjected in flight. The wind tunnel permits the experimental investigation of straight flight, but the very important cases of curvilinear flight and flight through squall lines cannot be reproduced there. For a reasonable duplication of such flight maneuvers, it becomes necessary to resort to another means of aerodynamic research, the whirling arm. This apparatus has been almost entirely discarded in aeronautical research, due to its inherent disadvantages as compared with the wind tunnel, and the difficulties encountered in obtaining exact measurements. These difficulties are: first, the additional air currents superimposing themselves upon the desired relative movement of the model fixed to such a whirling arm; and second, the high centrifugal forces to which turning models are subjected.

Since it becomes necessary to measure such

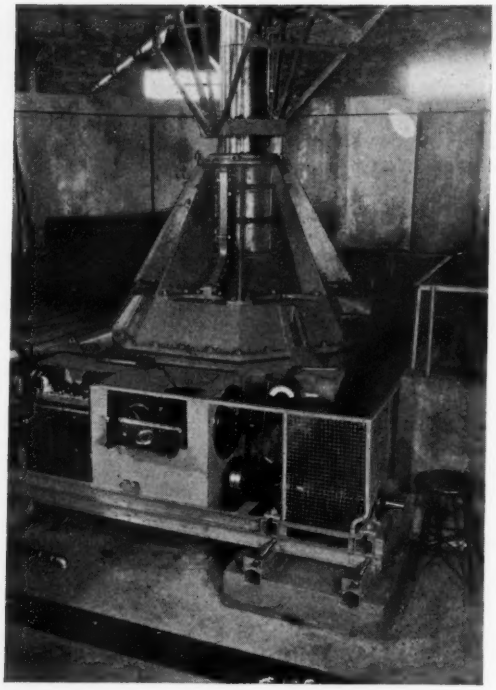

FIG. 1a. Whirling arm at the Daniel Guggenheim Airship Institute—drive and central part.

flight conditions of airships, an attempt has been made at this Institute to overcome the difficulties of the whirling arm as far as possible. In the construction which is shown in Figs. 1 and 2, the model moves through the center of a closed round channel of 20 foot height and a width which is variable between 16 and 20 feet, at the end of an arm 32 feet in radius, at a speed up to 170 m.p.h. (75 m/sec.). This speed is reached at an angular velocity of 75 r.p.m. of the arm. The installation of the inner wall of this channel prevents the creation of radial currents by the pumping effect of the turning arm. The size of the channel itself prevents convection currents of disturbing magnitude. The tangential swirl is cut out by a number of wire screens covering the cross section of the channel in several planes. A sufficient opening has been provided in these screens for the passage of the model and the arm. Airship models will be up to 12 feet in length, giving a Reynolds number

$$[\text{R.N.}]_e = \frac{\text{velocity} \times (\text{volume})^{1/3}}{\text{kinematic viscosity}}$$

of about $4.5 \times 10^6$. The whole installation permits tests with an accuracy similar to that of a wind tunnel, insofar as only wall corrections must be applied to the test results. The air conditions in this channel have been checked by means of Pitot tubes and hot wire anemometers at the maximum speed of the arm. A tangential velocity of approximately one percent of the velocity of the model was measured when the arm carried an inclined flat plate which had an equivalent drag area

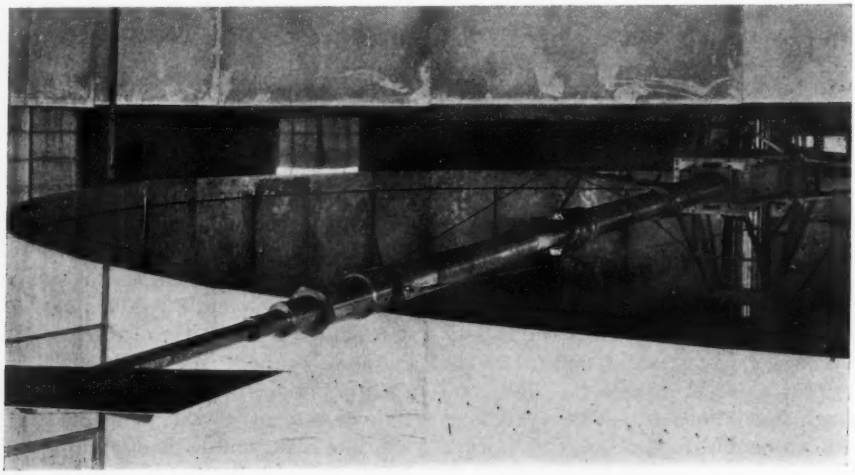

FIG. 1b. The whirling arm, extending through the slot in the inner wall of the round channel, carrying at its end a flat plate used for the investigation of swirl in the channel.

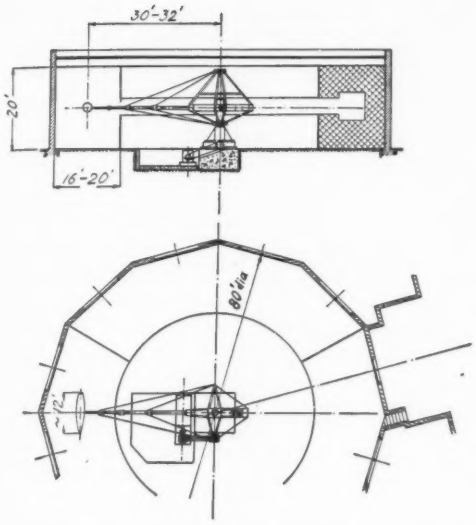


FIG. 2. Side and top view of the whirling arm. Three wire screens have been installed. The wire screen has a resistance coefficient of about 0.5, according to tests made at the Goettingen Versuchsanstalt.

$$A_D = D/q = 0.1 \text{ ft.}^2,$$

where $q$ = impact pressure; $D$ = drag.

For the measurement of pressure distributions on the turning model, the pressure holes are connected with a multiple tube manometer mounted on the turning shaft close to the center (see Fig. 3). The other ends of the manometer tubes are connected to a line turning with the arm and extending out approximately to the center of the model. The corrections which must then be applied involve only the small value of the centrifugal force on an air column of the radial length between the center of the model and the pressure opening. These corrections can be calculated. The pressure distribution is recorded on sensitive paper, as shown in Fig. 3.

A six-component balance system is being developed for the measurement of forces, in which the extension of the suspension wires is recorded by glass-scratching instruments. This suspension should at the same time give a rigid connection between the model and the arm and permit the measurement of shocks when the model enters artificial gusts. This latter possibility is provided for, because it is intended in the further development of this whirling arm to duplicate squall lines by blowing an air current upward through a section of the channel. The model used for force measurements must of course be very light and must be balanced in such a way that the effect of centrifugal forces on the registered forces is negligible.

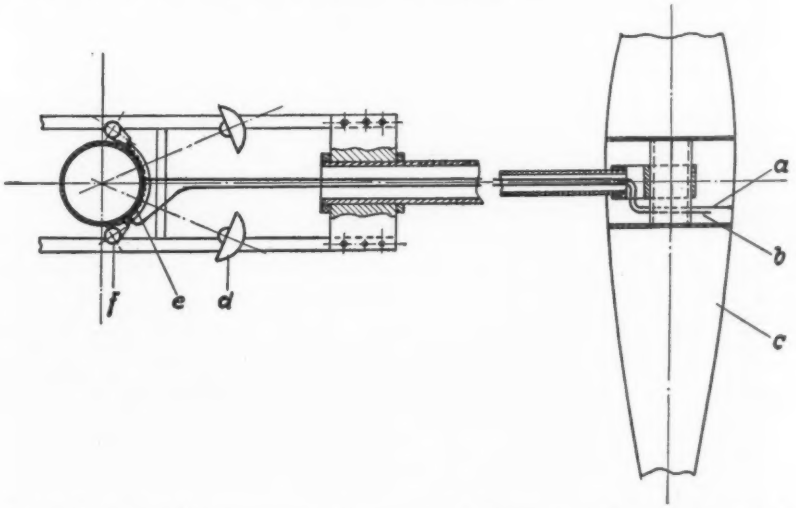


FIG. 3. Set-up for the measurement of pressure distribution on models rotating with the whirling arm. (a) connecting tube between pressure hole and manometer; (b) tube between manometer and center of model; (c) model; (d) lights used for the exposure of sensitive paper behind multiple tube manometer; (e) tubes of manometer comb; (f) containers for sensitive paper.

# A Belt Method of Representing the Ground

ALEXANDER KLEMIN, *New York University*
(Submitted August 7, 1934)

IN the July issue of the Journal, Professor Stalker described his ingenious method of placing a reflection plate representing the ground under alternate suction and ejection to remove the boundary layer and to reduce the vertical component of flow to zero. Certainly this constitutes an advance over both the mirror method and the ordinary ground board method. But some objections may perhaps be offered:

1. The surface of the reflector plate is broken up by the suction and ejection openings, which certainly does not make for accuracy.

2. The alternate suction and ejection make for a local circulatory flow which is undesirable.

3. The boundary layer is apparently not reduced to zero, as it should be.

4. Every new model tested in itself modified the boundary layer of the ground board, and therefore each new model should be accompanied by fussy and difficult measurements of boundary layer velocities.

5. It is evident that some adjustment of suction and ejection effect along the length of the plate would be desirable.

6. The apparatus is not perfect "theoretically."

7. It is frequently desirable to test models of automobiles, trains, etc., at varying wind speeds to determine an exponent of scale effect. In such a case it would be necessary to make painstaking adjustment of the suction and ejection to correspond with each tunnel speed.

If it is really desirable to secure a standard reflector plate method, then the solution first proposed by Eiffel, some twenty years back, of a moving belt to represent the ground appears to be more attractive. Eiffel failed to make his moving belt function properly due to vibration and shifting of position.

Such a belt has now been made to function (after four months of "cut and try") in the 9 foot wind tunnel of New York University and tests have been made up to speeds of 70 miles an

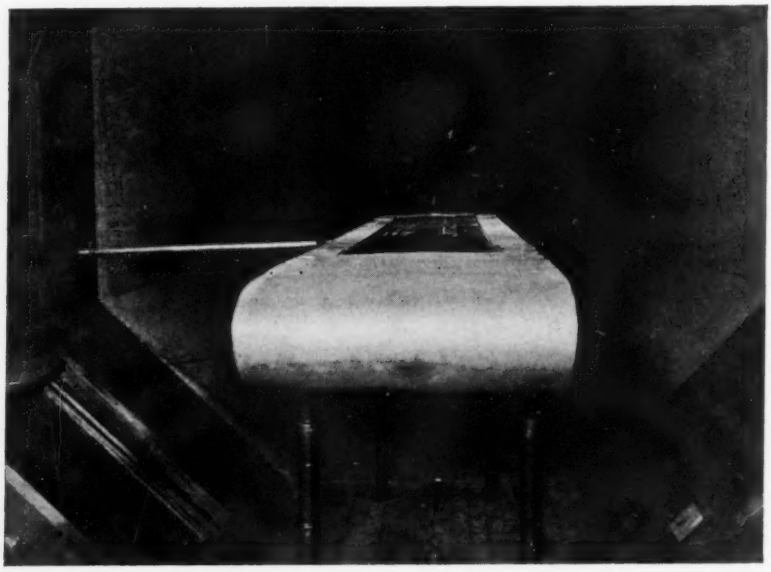

FIG. 1.

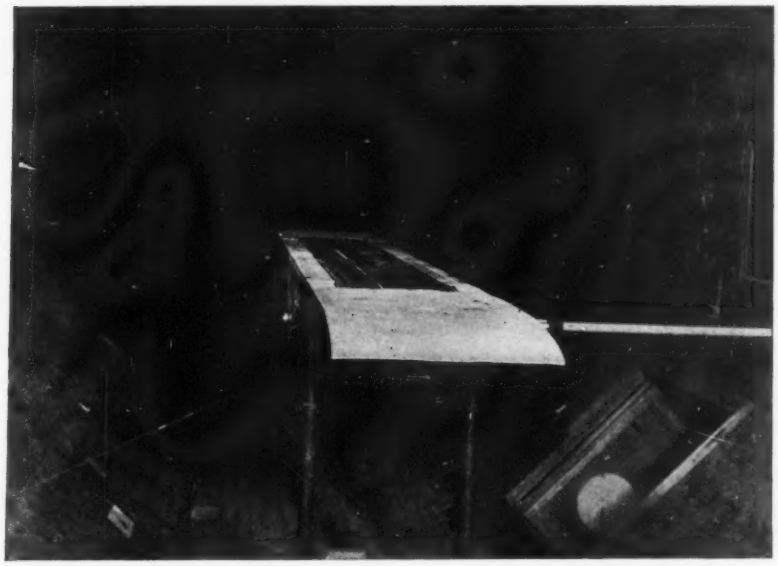

FIG. 2.

hour with no flapping, vibration or crowning. That the surface of the belt remained flat has been demonstrated by visual observation, and by suspending the wheels of a model only 1/64th of an inch from the belt with steady readings on the tunnel balance. Any contact between belt and model, or any shifting of the belt would of course have changed the balance readings.

The apparatus is illustrated in Figs. 1 and 2. The belt now in use is 78″ long and 12″ in width, and could be increased in dimensions without difficulty. It is driven by an electric motor placed outside the tunnel, whose speed can be adjusted so as to make wind speed and ground speed exactly equal. Ball bearing rollers of generous diameter are employed, and the joint in the belt is carefully constructed so as to present no break or disturbance in the surface of the belt. The belt only requires lateral guides at the rollers themselves. The distance between the centers of the rollers must be adjustable, so that the belt is neither too loose nor too taut. The ground board is of course suitably recessed to take the belt and a shield is provided at the front end of the belt. Set up and operation of the belt require care but offer no particular difficulty in experienced hands.

Results of tests made with the belt substantiate the general theory that the elimination of the boundary layer increase the resistance of a model as compared with the ordinary ground board method.

## Election of Fellows

With the election of the Fellows listed below, the complement of fifty for this class of membership is filled until 1935. Ten additional Fellows may be elected hereafter each year.

Edwin E. Aldrin,
G. M. Bellanca,
W. R. Gregg,
Major Leslie MacDill,
Robert R. Osborn,
Prof. F. W. Pawlowski,
Dr. Th. Theodorsen,
Ralph H. Upson,
Comdr. R. D. Weyerbacher.

## Members Visit Yachts *Endeavour* and *Rainbow*

UPON the invitation of T. O. M. Sopwith, a member of the Institute, a group of his fellow members visited the yacht *Endeavour*, at Newport, on Wednesday afternoon, August 29th. After having the special applications of aerodynamics to the construction of the yacht explained by Mr. Sopwith and Charles E. Nicholson, the designer of the yacht, the party were invited by Harold S. Vanderbilt to make a similar inspection of the yacht *Rainbow*. W. Starling Burgess, the designer of the *Rainbow*, who in 1910 was constructing airplanes, gave the party an interesting description of the many aeronautical innovations he had introduced.

## Dinner to T. O. M. Sopwith

A DINNER was given by the Institute in honor of T. O. M. Sopwith, a member, and challenger for the America's cup, at the University Club in New York, on Friday, September 28th.

A reception was held for Mr. Sopwith immediately preceding the dinner. Two hundred members and guests attended.

Charles L. Lawrance, President of the Institute, was toastmaster. The speakers were: C. R. Fairey, M.B.E., President of the Royal Aeronautical Society; Hon. Clark Howell, Chairman of the Federal Aviation Commission; Lt. Col. J. T. C. Moore-Brabazon, M.C., M.P., President-elect of the Royal Aeronautical Society; Rear Admiral E. J. King, U.S.N., Chief, Bureau of Aeronautics, Navy Department; Brig. Gen. Oscar Westover, U.S.A., Asst. Chief, Air Corps, War Department, and Mr. Sopwith.

Hon. F. H. LaGuardia, Mayor of the City of New York, was absent due to illness. A letter of regret from the Mayor was read by Mr. Lawrance. F. William Zelcer, Deputy Commissioner of Docks in charge of Aviation, spoke on the Mayor's behalf.

The members of the dinner committee were: Sherman M. Fairchild, Grover Loening, Glenn L. Martin, George J. Mead, Thomas A. Morgan, Dr. S. A. Reed.

Among those present at the guest tables were: Vincent Bendix, S. S. Bradley, C. H. Colvin, L. K. Comstock, Rear Admiral H. I. Cone, C. W. Deeds, Capt. T. B. Doe, A. V. de Forest, Major J. H. Doolittle, Sherman M. Fairchild, Major Lester D. Gardner, L. R. Grumman, Hon. Harry F. Guggenheim, H. M. Hanshue, Dr. J. C. Hunsaker, R. F. Hoyt, C. S. Jones, Dr. J. H. Kimball, Prof. Alexander Klemin, Rear Admiral E. S. Land, Dr. G. W. Lewis, Grover Loening, Glenn L. Martin, L. C. Milburn, E. D. Osborn, A. A. Priester, Dr. S. A. Reed, Calvin Rice, Captain E. V. Rickenbacker, J. P. Ripley, Richard W. Robbins, Leighton Rogers, F. H. Russell, I. I. Sikorsky, E. A. Sperry, Wm. B. Stout, E. P. Warner, J. A. C. Warner, Harold P. Westman, Comdr. R. D. Weyerbacher, Gar Wood, T. P. Wright.

## Necrology

Hermann Glauert, a Scientific Member of the Institute, died on August 4, 1934, in England. Mr. Glauert was a Fellow of the Royal Aeronautical Society and the Royal Society.

Hermann Glauert was born in Sheffield on October 4, 1892, and was the son of Mr. Louis Glauert. He was educated at King Edward VII School, Sheffield, and Trinity College, Cambridge. He joined the staff of the Royal Aircraft Establishment in 1916, where he was engaged on aerodynamical research until his death.

Hermann Glauert made many important contributions to the science of aerodynamics. He was the author of numerous Reports and Memoranda of the Aeronautical Research Committee dealing with airfoil and airscrew theory, performance, stability and control of airplanes, and the theory of the autogiro. His work, "The Elements of Aerofoil and Airscrew Theory," published in 1926, is a standard work on the subject.